

Results from Pb+Pb collisions at the LHC

Constantin Loizides
(LBNL/EMMI)

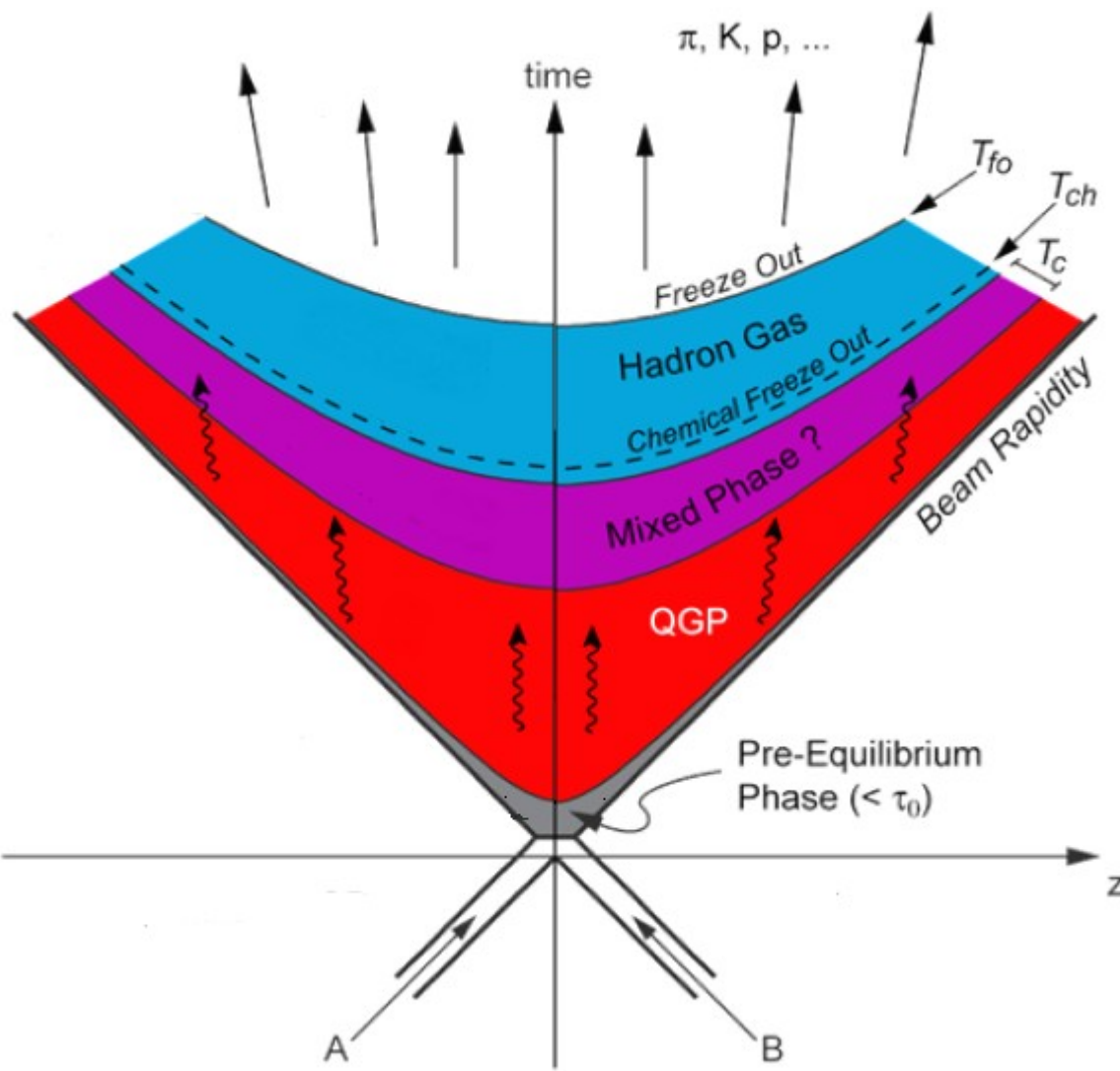
05 June 2012

Physics at the LHC 2012

Vancouver, BC

A wide-angle photograph of the Vancouver skyline at night. The city is brightly lit with numerous lights from buildings and street lamps. In the background, the snow-capped mountains of the Coast Range are visible under a dark, cloudy sky.

Heavy-ion standard reaction model



Global properties

Kinetic freeze-out

Chemical freeze-out

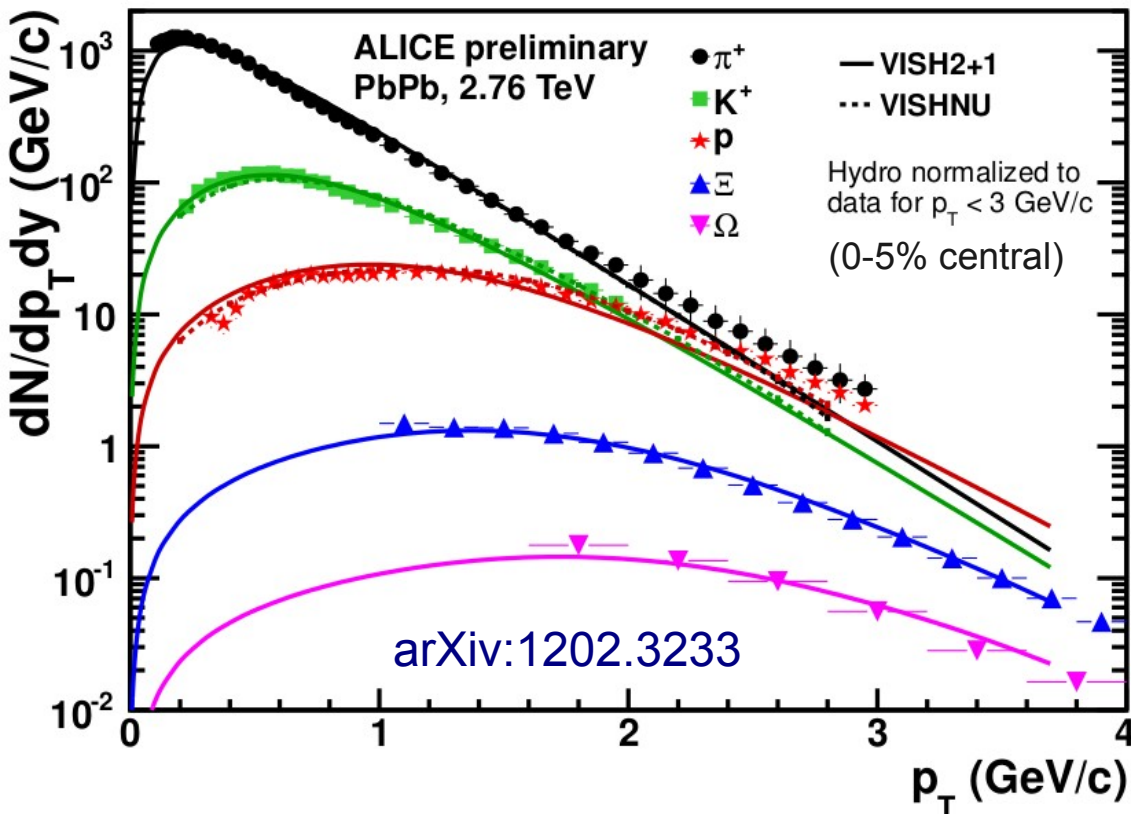
Collective flow

Hard probes
(jets, heavy flavor)

Order discussed in talk

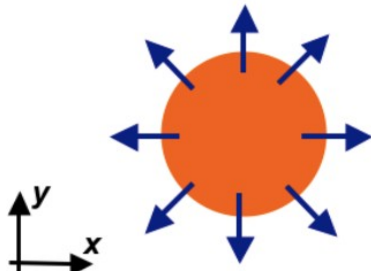
“Rewind dynamical evolution” to access QGP by studying many observables with different sensitivity to the stages of the collision

Radial flow and kinetic freeze-out



- Shape for particles with different masses indicate radial flow
- Hydrodynamical calculations describe the data
- Fits assuming a boosted thermal source with a common temperature and radial velocity

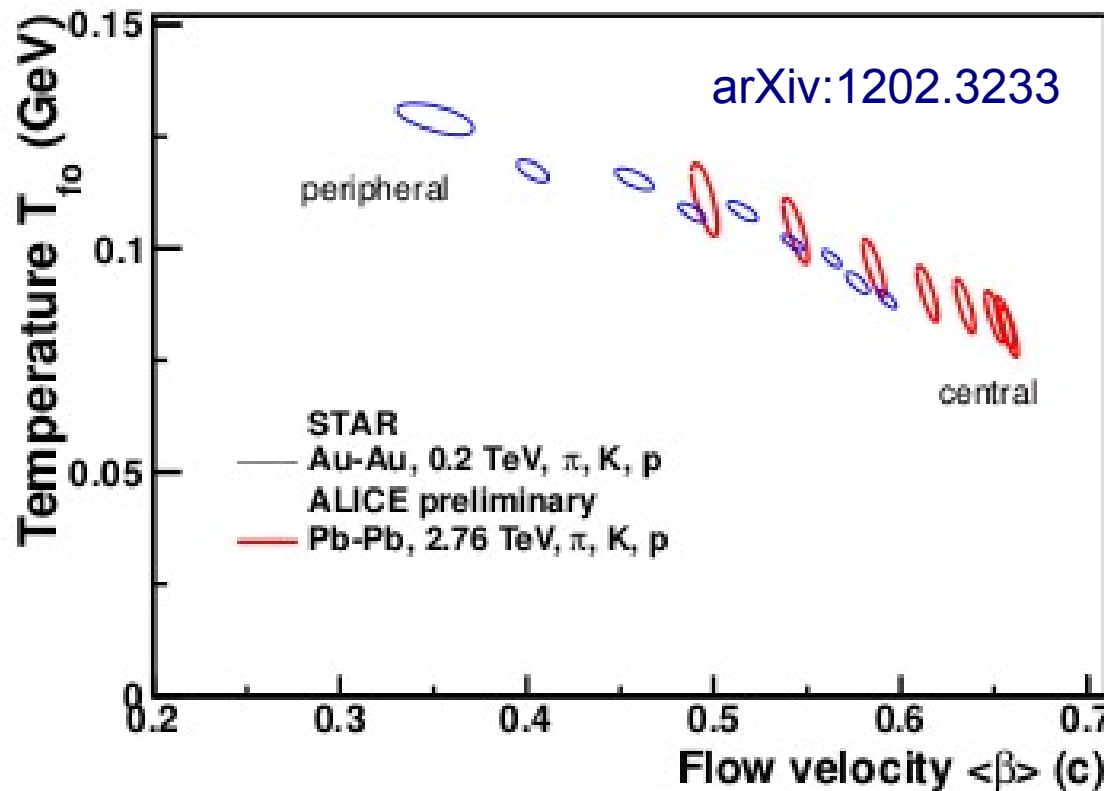
Radial flow



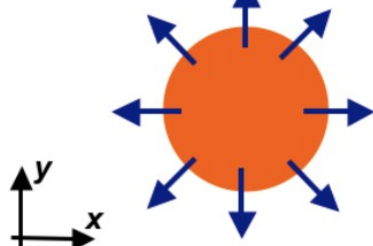
$$p_T^{flow} = p_T + m \beta_T^{flow} \gamma_T^{flow}$$

Radial flow and kinetic freeze-out

4



Radial flow

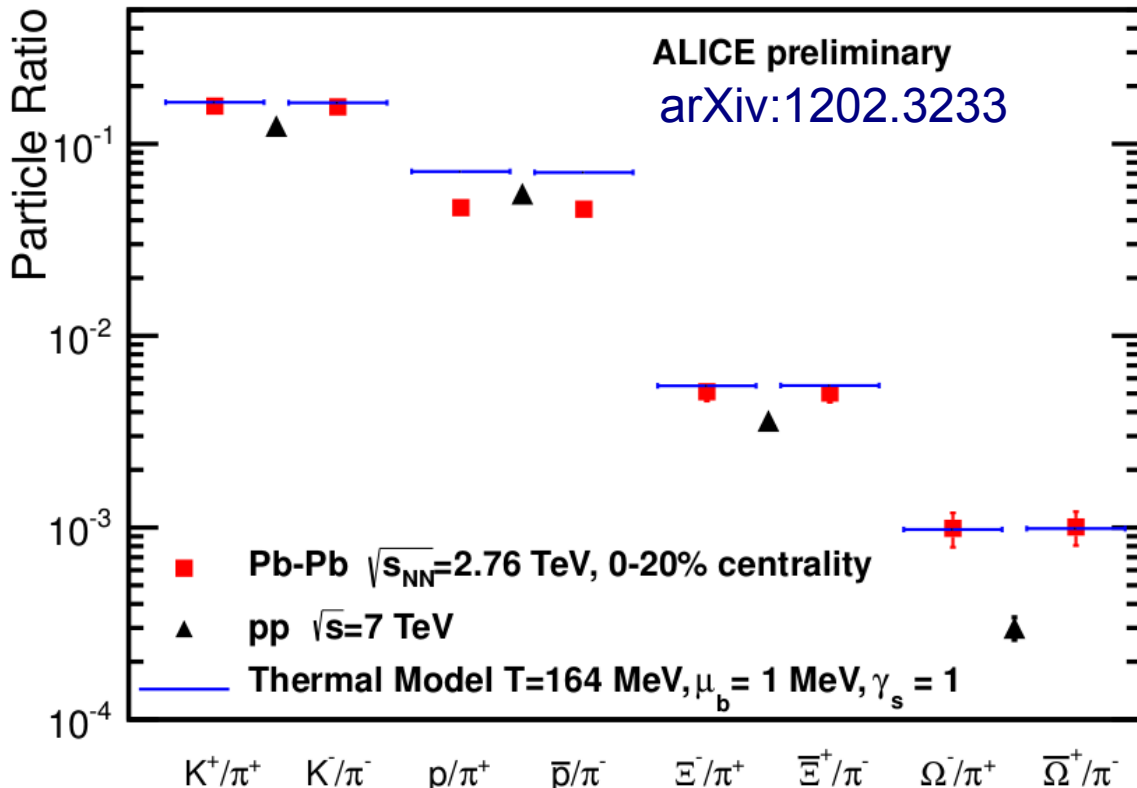


$$p_T^{flow} = p_T + m \beta_T^{flow} \gamma_T^{flow}$$

- Shape for particles with different masses indicate radial flow
- Hydrodynamical calculations describe the data
- Fits assuming a boosted thermal source with a common temperature and radial velocity
 - Strong radial flow up to $\beta_{LHC,central} = 0.66c$
 - $\beta_{LHC,central} = 1.1 \beta_{RHIC,central}$
 - Kinetic freeze-out $T_{fo} = 80-100$ MeV
 - Up to ~25% higher mean p_T at the same $dN/d\eta$

Particle ratios and chemical freeze-out

5

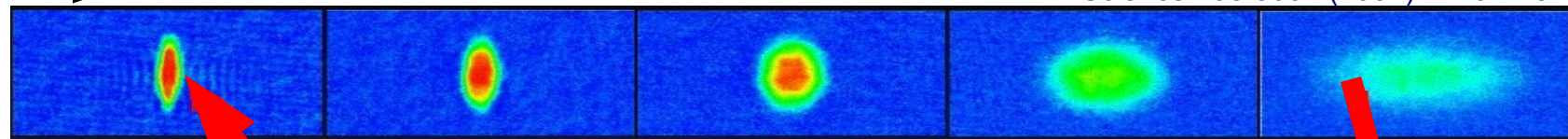


- Statistical (thermal) model
$$N_i \propto V \int \frac{d^3 p}{2 \pi^3} \frac{1}{e^{(E_i - \mu_B B_i)/T_{ch}} \pm 1}$$
 - Chemical potential depends on baryon number, strangeness and isospin
 - Two parameters: T_{ch} , μ_B
- Obtain: $T_{ch} \approx 164$ MeV $\approx T_c$
 - In agreement with expectation from lattice
 - Holds for $\sqrt{s_{NN}} > 10-20$ GeV
 - Strangeness enhancement in AA well described
 - Proton/pion ratio at the LHC to be understood

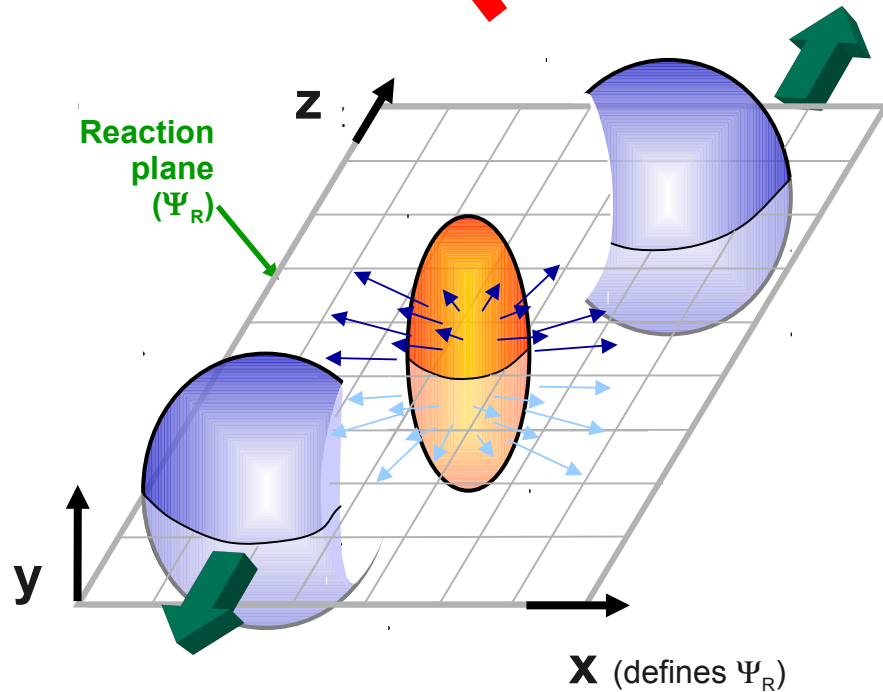
Initial and final state anisotropy

Time

Science 298 5601 (2002) 2179-2182

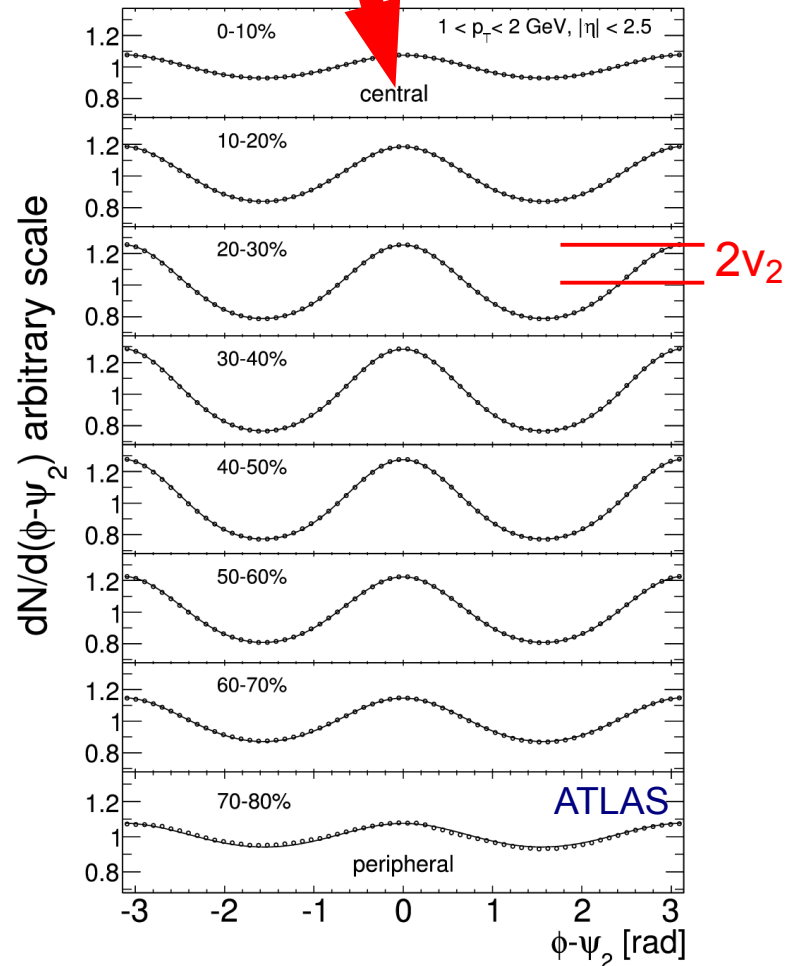


(self quenching)



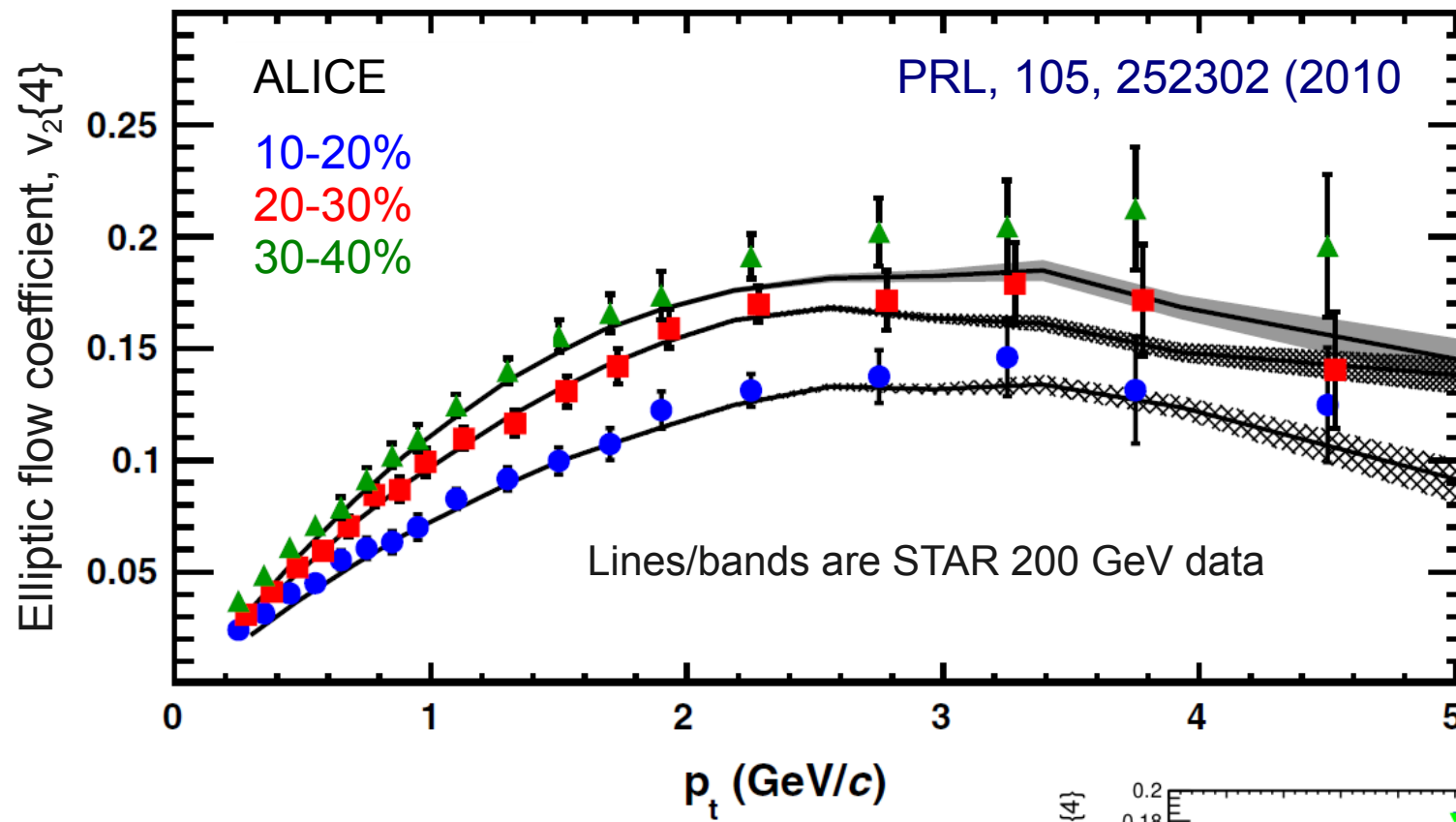
Initial spatial anisotropy:
eccentricity ϵ

Interactions
present early

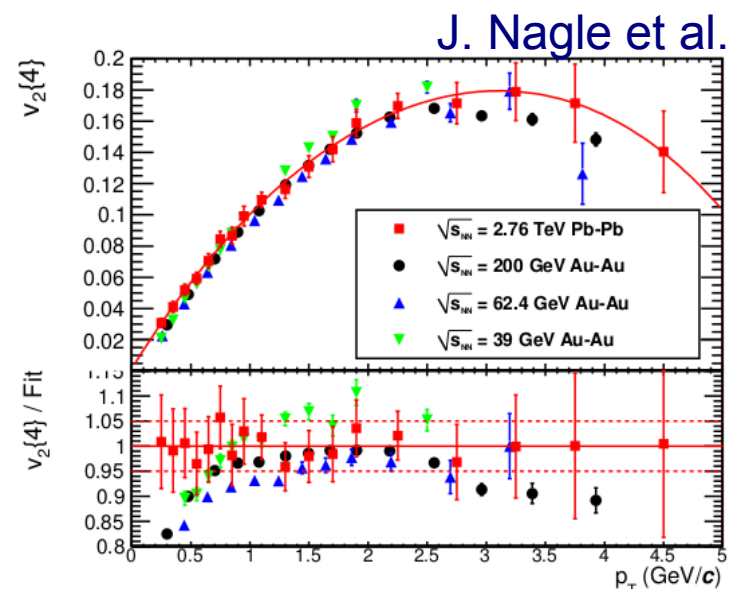


Momentum space anisotropy:
elliptic flow $v_2 = \langle \cos(2\phi - 2\Psi_R) \rangle$

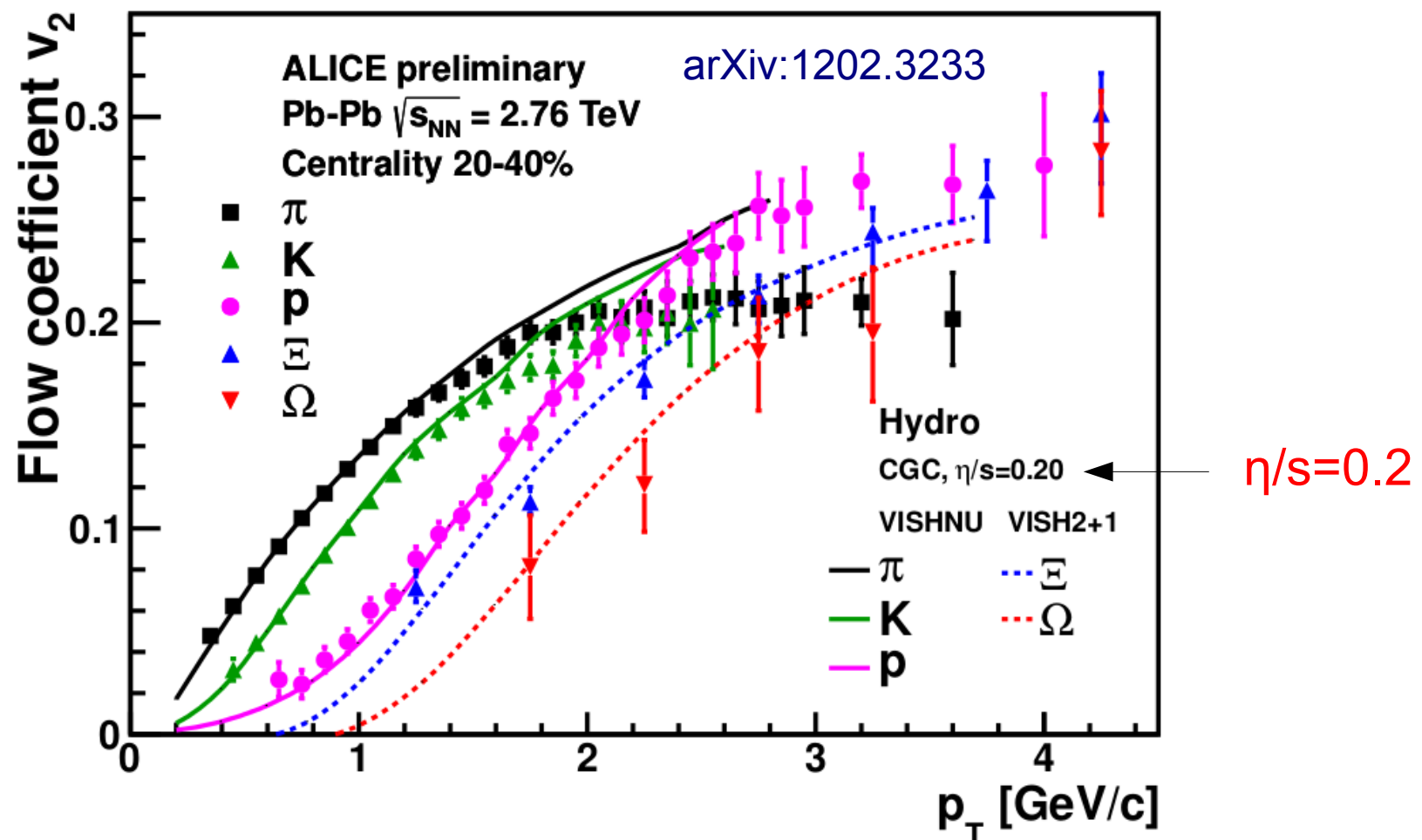
Charged particle elliptic flow



Observe $v_2(p_T)_{\text{LHC}} \approx v_2(p_T)_{\text{RHIC}}$,
despite factor 14 increase in cms energy!
(Integrated v_2 30% larger due to radial flow)

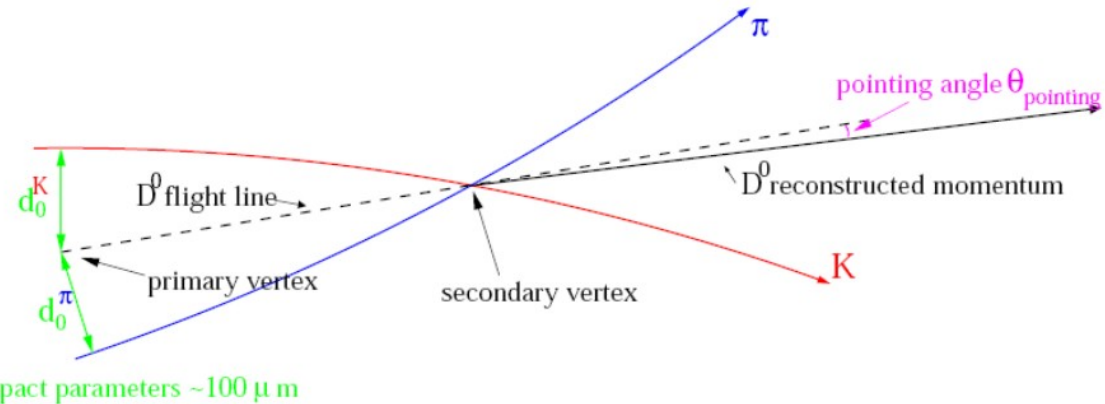
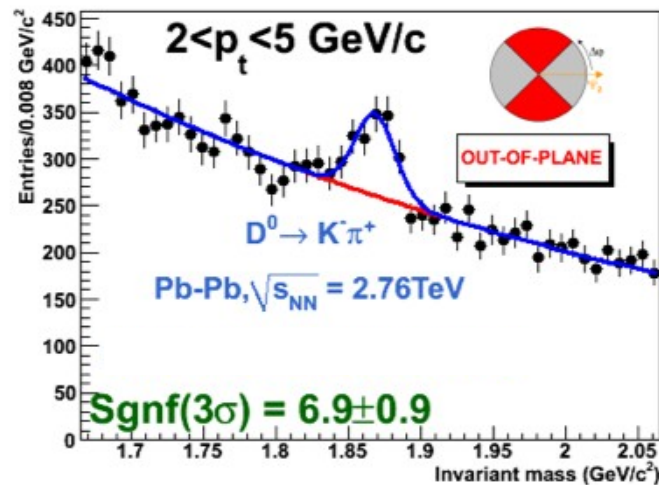
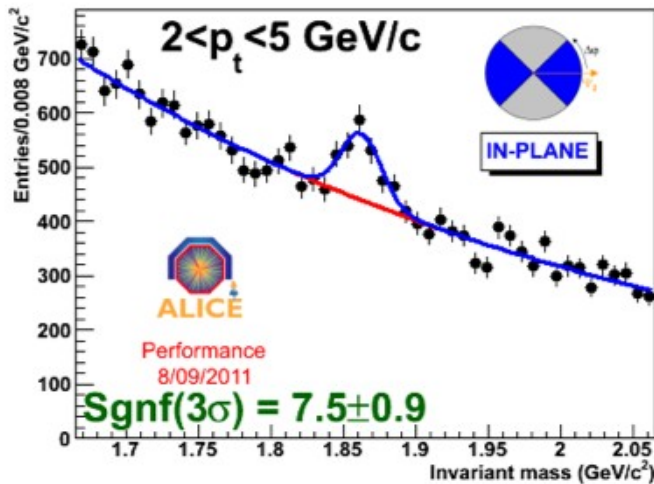


Identified particle elliptic flow



Observed mass ordering due to radial flow
 as predicted by hydrodynamical calculations

D meson elliptic flow

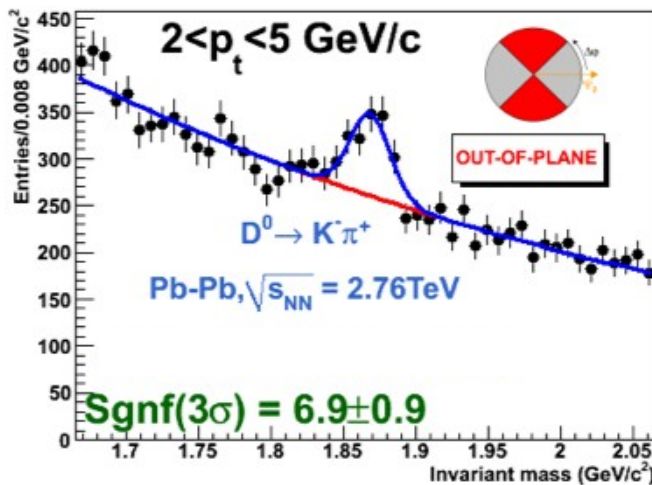
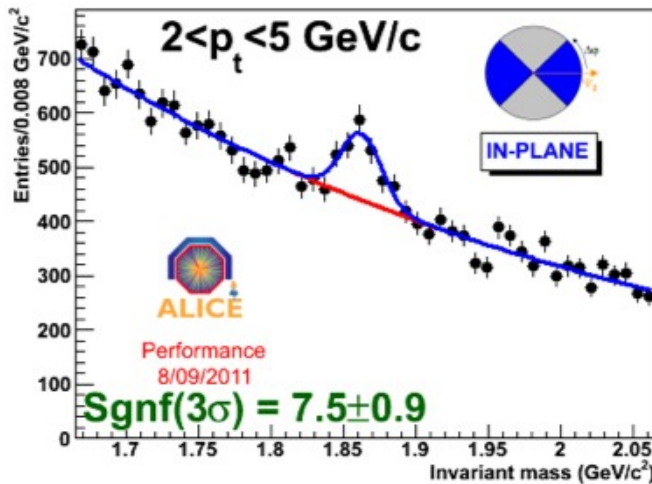


- Invariant mass analysis of fully reconstructed decay topologies (inc. PID) displaced from primary vertex
- Feed-down from B (10-15% after cuts) subtracted using FONLL
 - Conservative hypothesis on R_{AA} of D from B

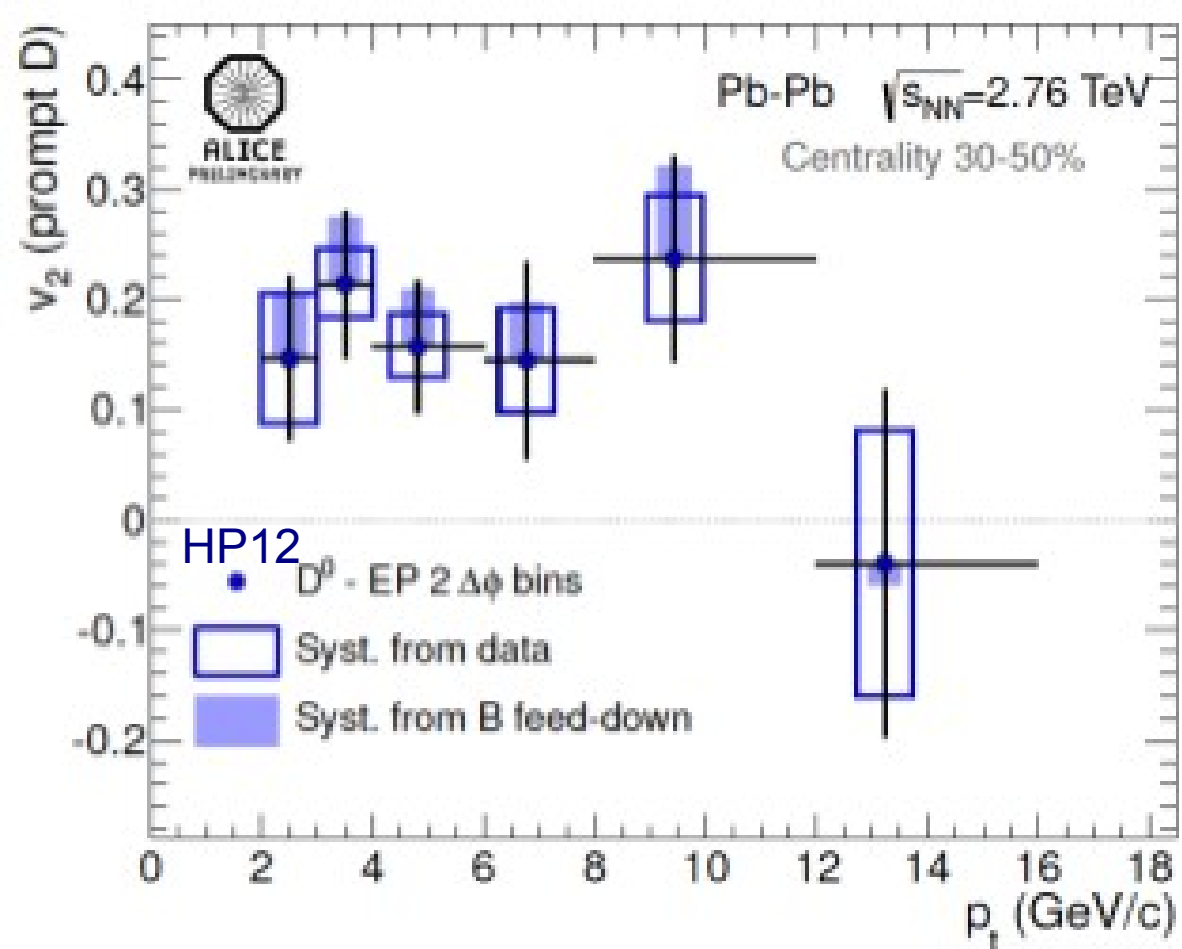
ALICE PID (see C.Zampolli Mon)

D meson elliptic flow

10

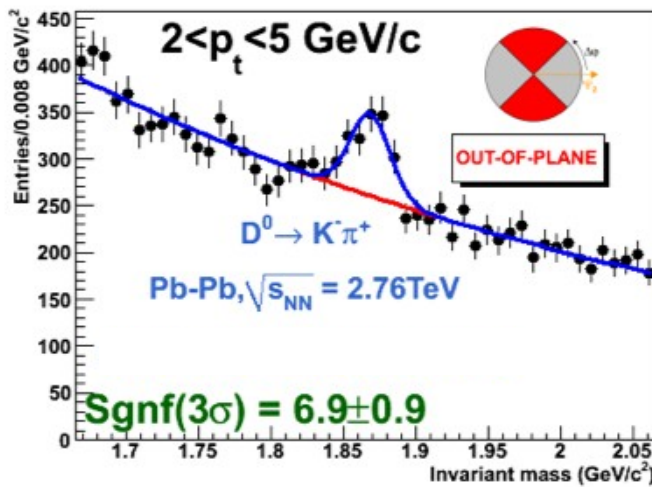
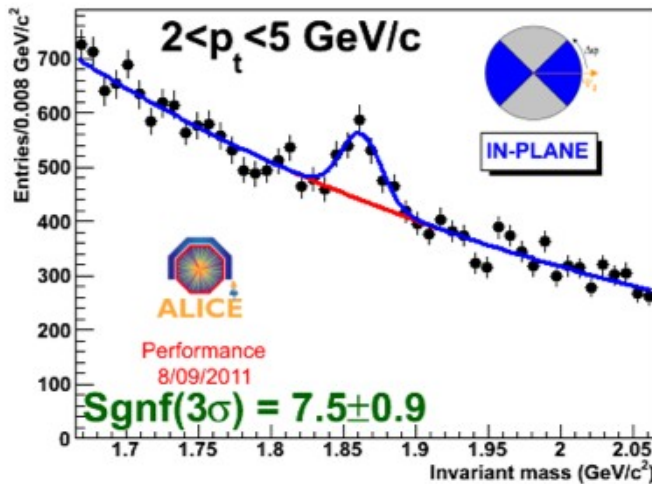


$$v_2 = \frac{\pi}{4} \frac{N_{\text{IN}} - N_{\text{OUT}}}{N_{\text{IN}} + N_{\text{OUT}}}$$

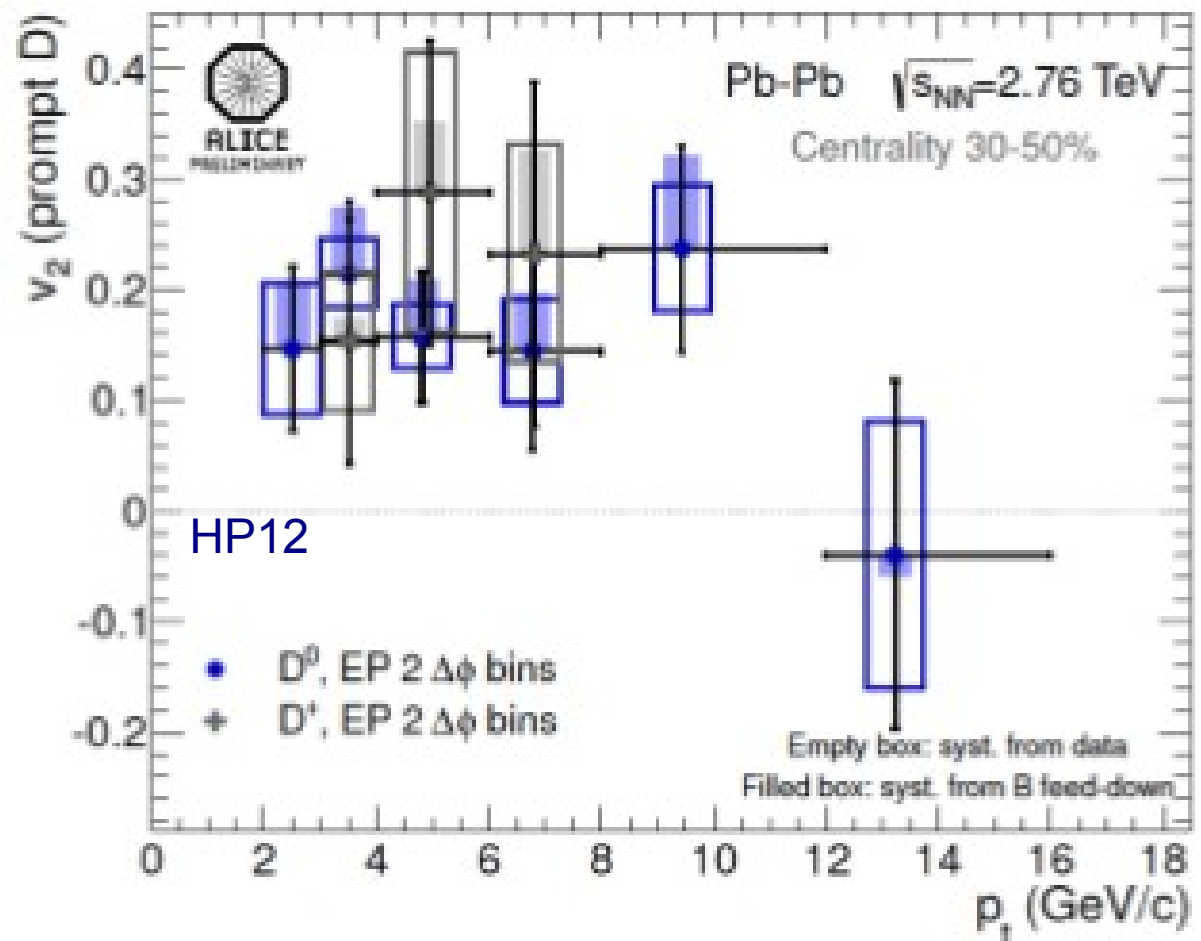


Even the charm mesons exhibit elliptic flow

D meson elliptic flow



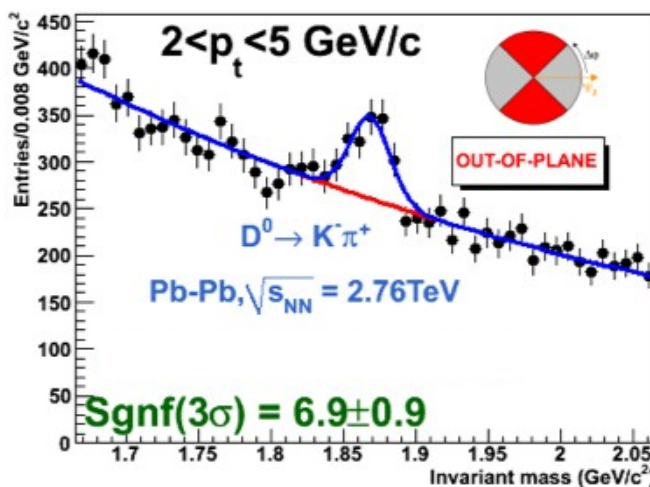
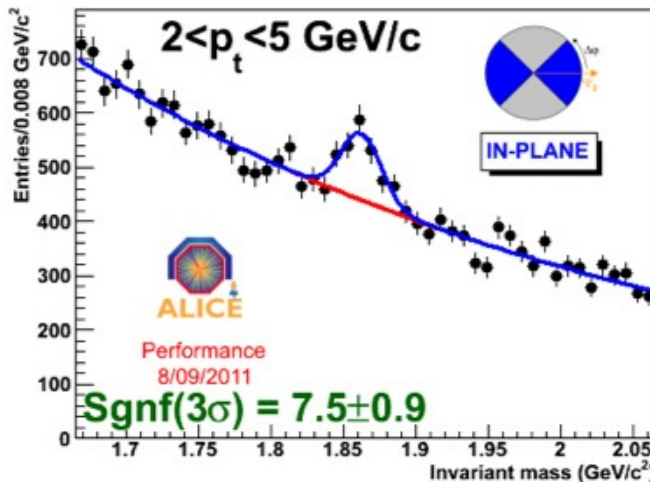
$$v_2 = \frac{\pi}{4} \frac{N_{\text{IN}} - N_{\text{OUT}}}{N_{\text{IN}} + N_{\text{OUT}}}$$



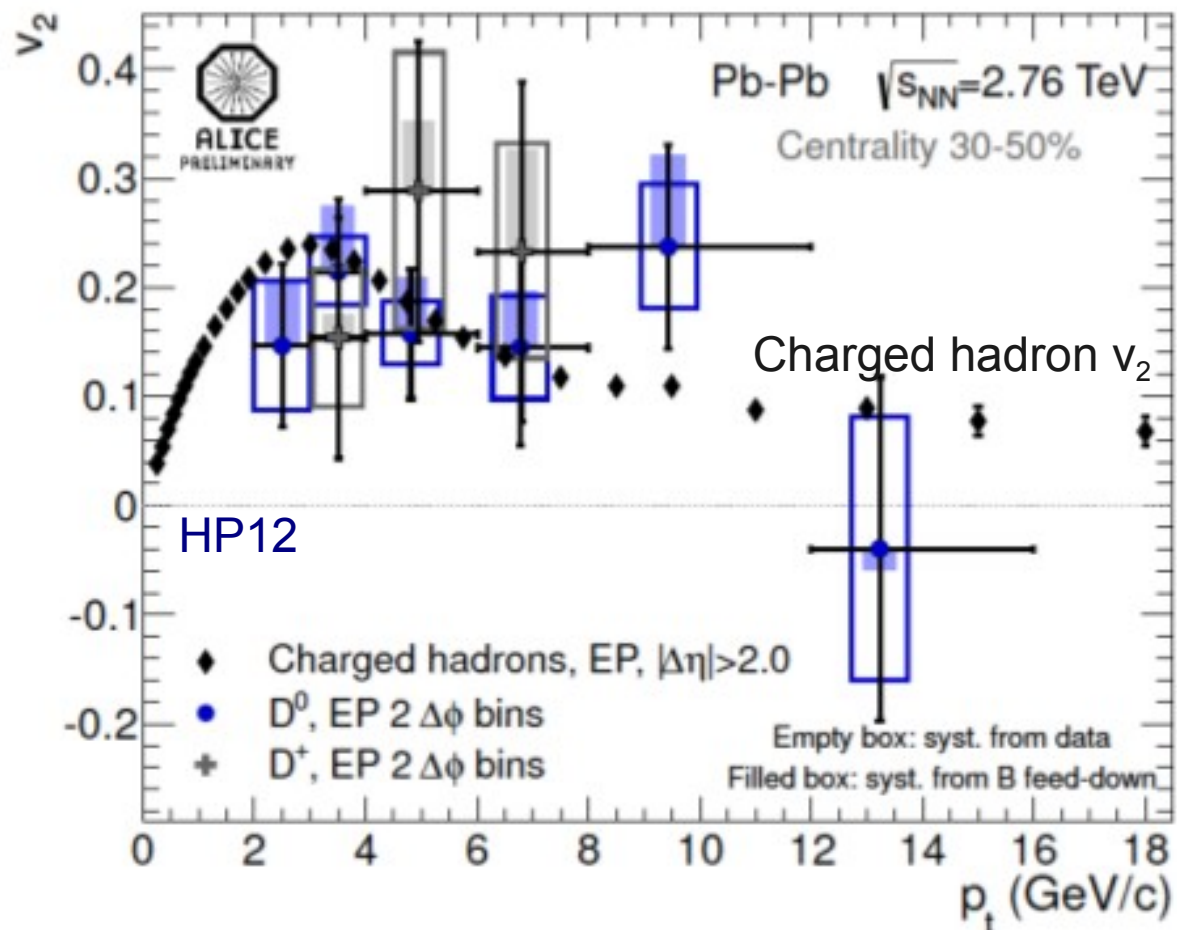
Even the charm mesons exhibit elliptic flow

D meson elliptic flow

12



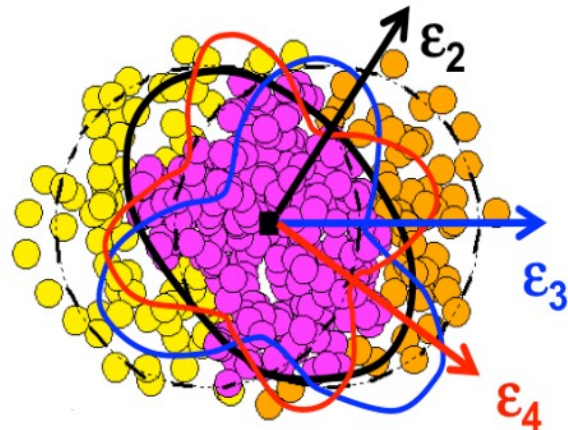
$$v_2 = \frac{\pi}{4} \frac{N_{\text{IN}} - N_{\text{OUT}}}{N_{\text{IN}} + N_{\text{OUT}}}$$



Even the charm mesons exhibit elliptic flow
(similar to the charged particle v_2)

Higher harmonics and viscosity

13



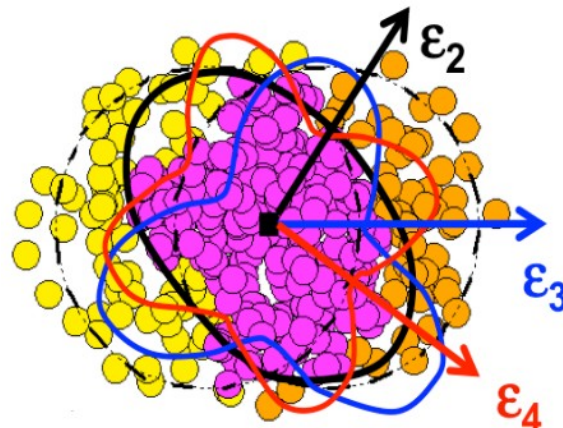
Alver, Roland

Initial spatial anisotropy not smooth, leads to higher harmonics / symmetry planes.

$$\frac{dN}{d\phi} \sim 1 + 2v_2 \cos[2(\phi - \psi_2)] + 2v_3 \cos[3(\phi - \psi_3)] \\ + 2v_4 \cos[4(\phi - \psi_4)] + 2v_5 \cos[5(\phi - \psi_5)] + \dots$$

Higher harmonics and viscosity

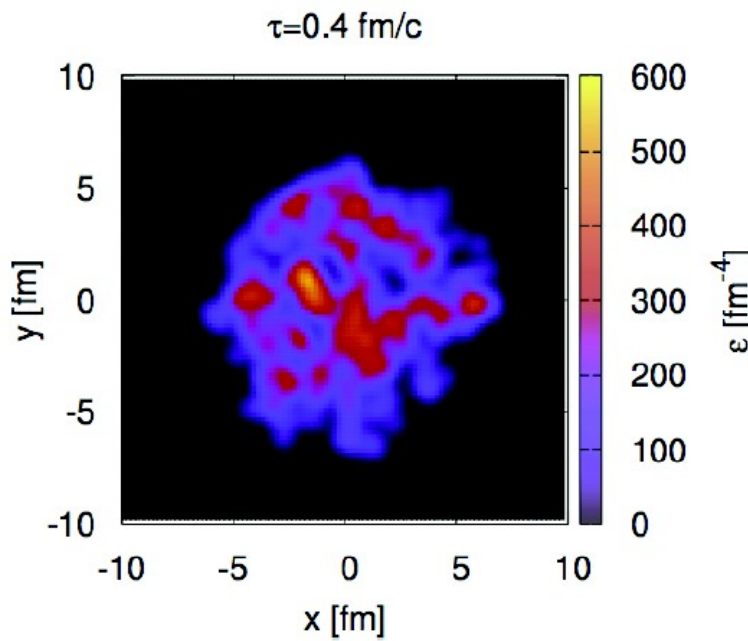
14



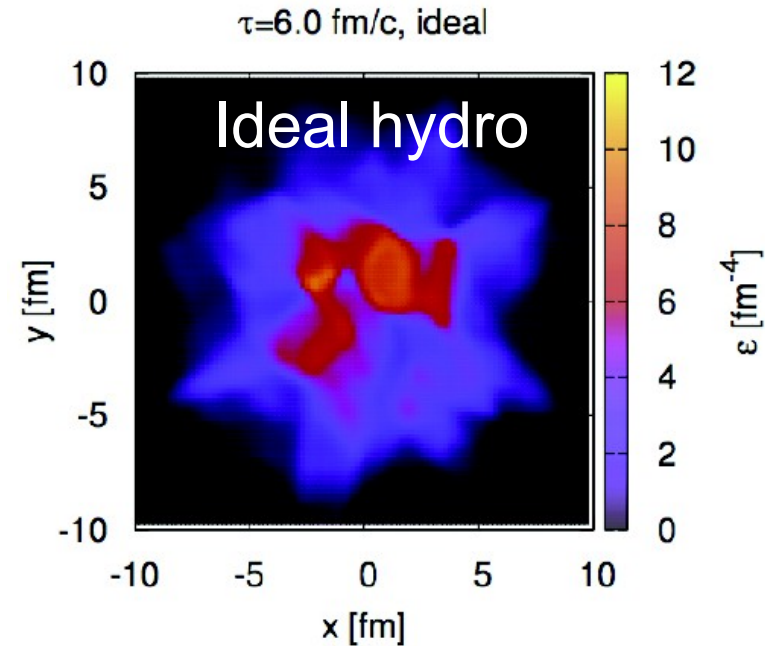
Alver, Roland

Initial spatial anisotropy not smooth, leads to higher harmonics / symmetry planes.

$$\frac{dN}{d\phi} \sim 1 + 2v_2 \cos[2(\phi - \psi_2)] + 2v_3 \cos[3(\phi - \psi_3)] \\ + 2v_4 \cos[4(\phi - \psi_4)] + 2v_5 \cos[5(\phi - \psi_5)] + \dots$$



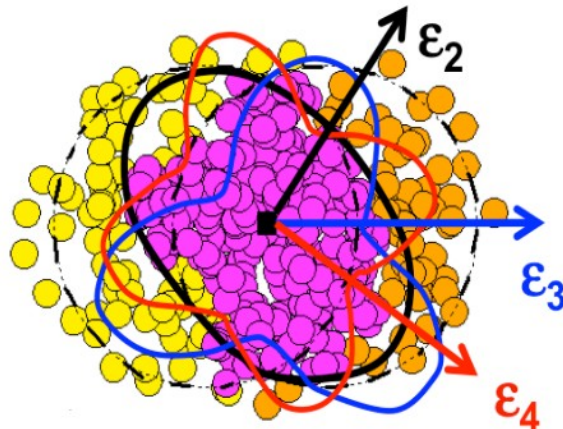
e-by-e hydro
B. Schenke et al.



Ideal hydrodynamical models preserves these “clumpy” initial conditions

Higher harmonics and viscosity

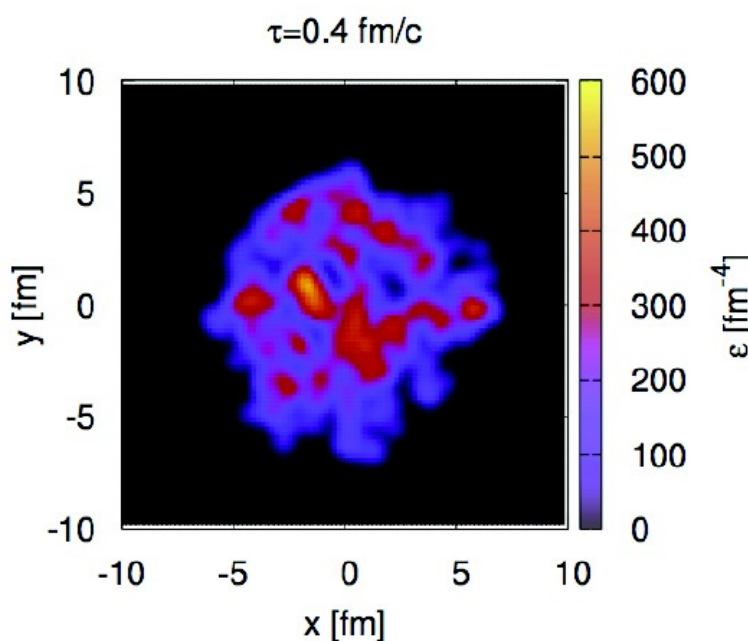
15



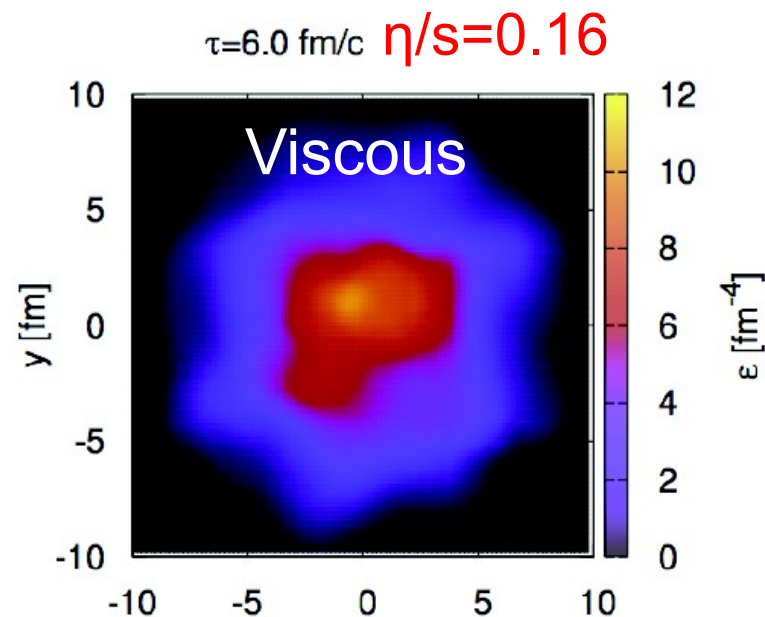
Alver, Roland

Initial spatial anisotropy not smooth, leads to higher harmonics / symmetry planes.

$$\frac{dN}{d\phi} \sim 1 + 2v_2 \cos[2(\phi - \psi_2)] + 2v_3 \cos[3(\phi - \psi_3)] \\ + 2v_4 \cos[4(\phi - \psi_4)] + 2v_5 \cos[5(\phi - \psi_5)] + \dots$$

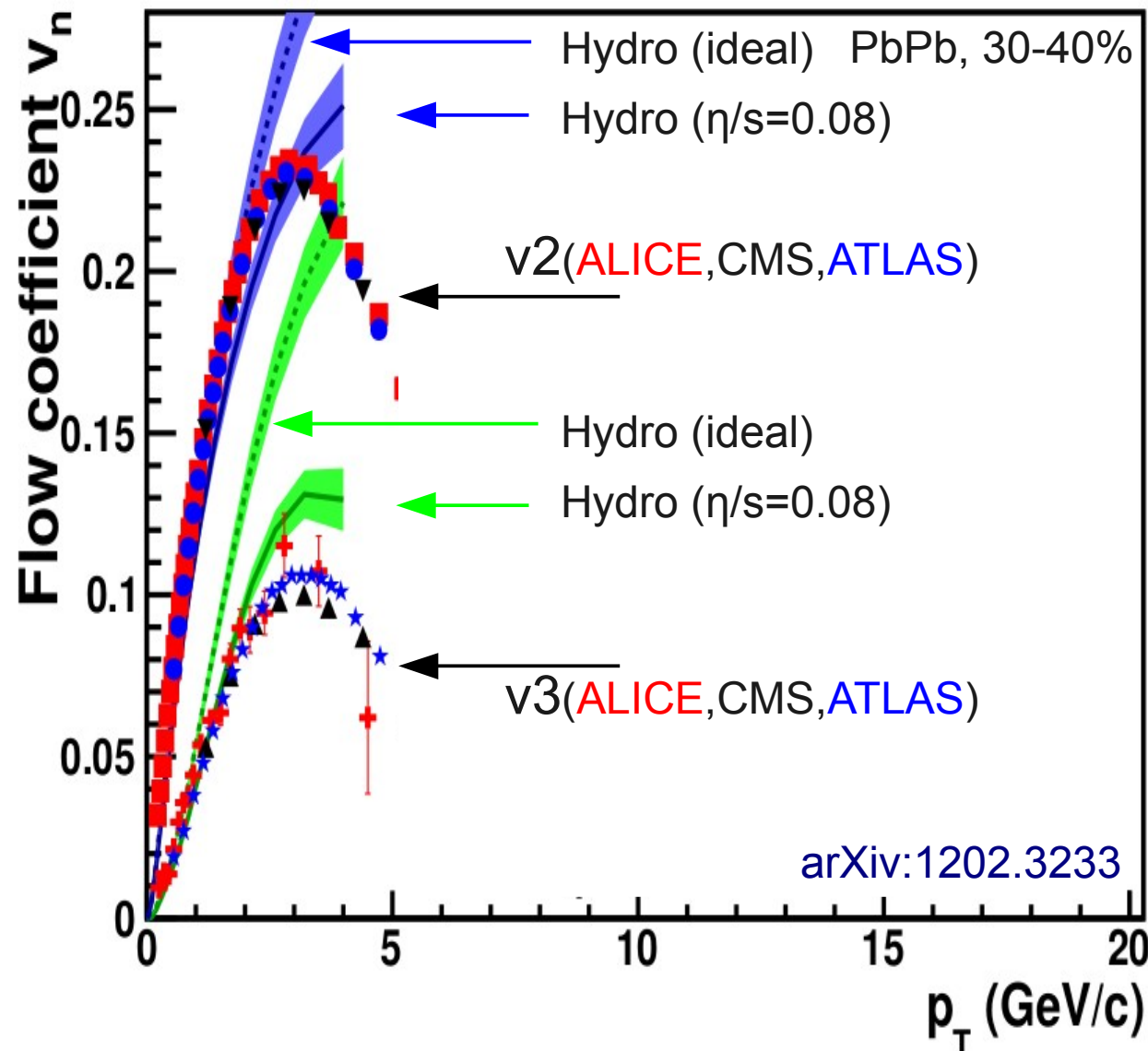


e-by-e hydro
B. Schenke et al.



Viscosity suppresses higher harmonics,
→ v_n provide additional sensitivity to η/s

Limits on η/s from charged particle v_2 and v_3 16



- Significant v_3 component
- Viscosity dissipates initial pressure gradients and reduces the collective flow
- v_3 provides additional constraints on η/s
- Current bound at LHC
 - $\eta/s < 2/(4\pi) = 2(\eta/s)_{\min}^{\text{ADS/CFT}}$

Qui, Shen, Heinz, PLB 707 (2012) 151

ALICE, PRL 107 (2011) 032301

ATLAS, PLB 707 (2012) 330

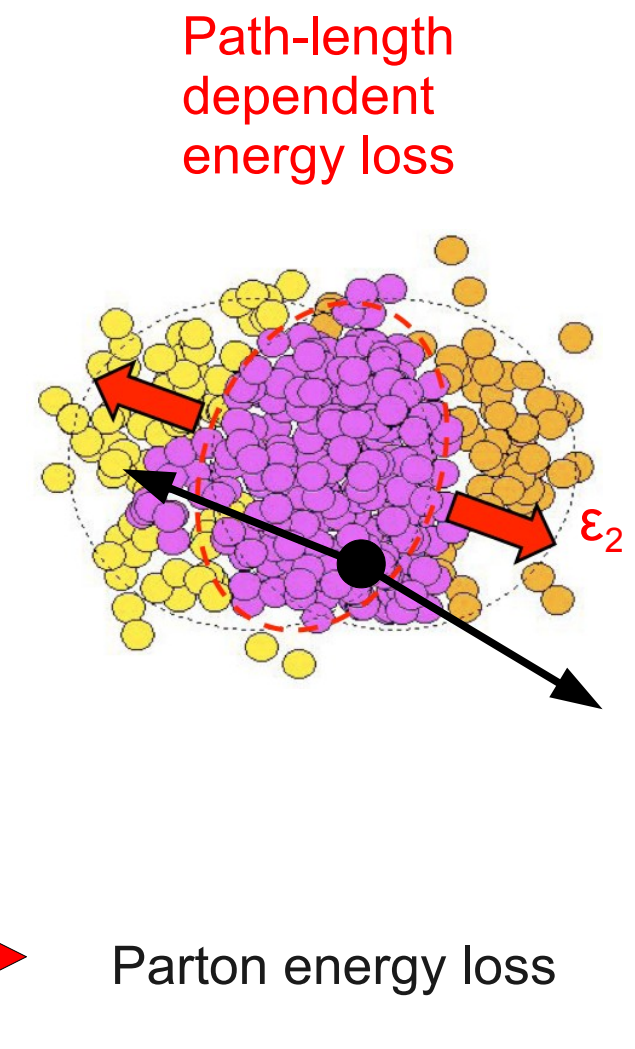
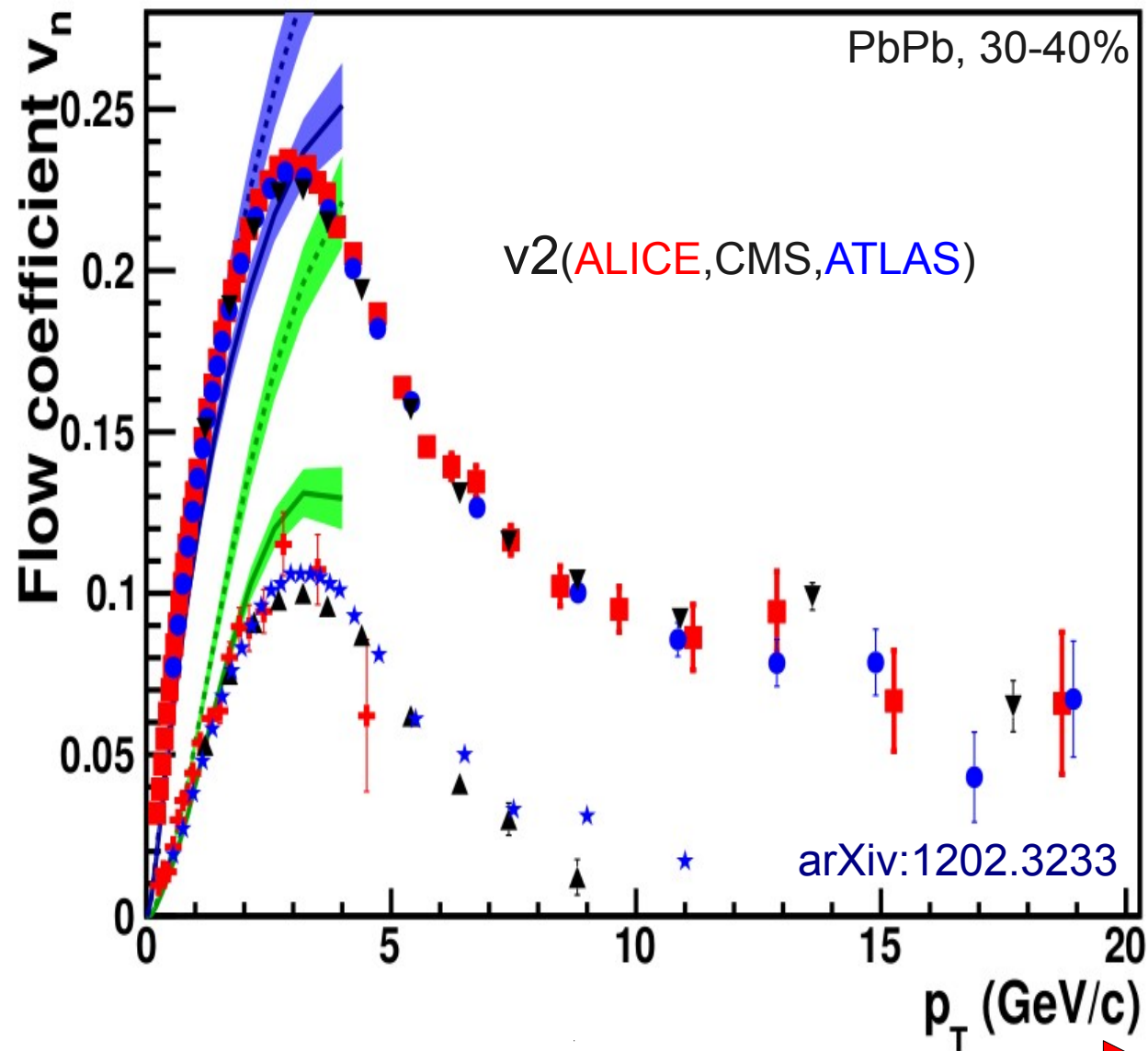
ATLAS, arXiv:1203.3087

CMS, arXiv:1204.1409

The quark-gluon plasma at the LHC is still a nearly perfect liquid

Soft, intermediate and hard p_T region

17



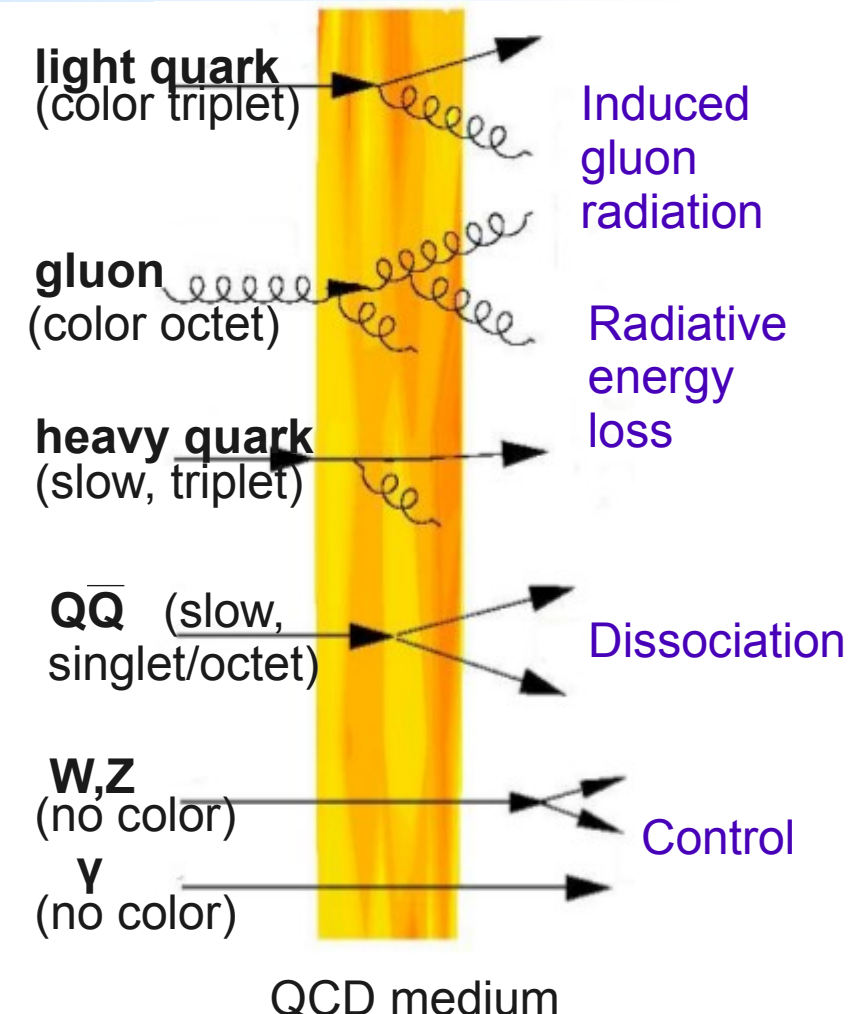
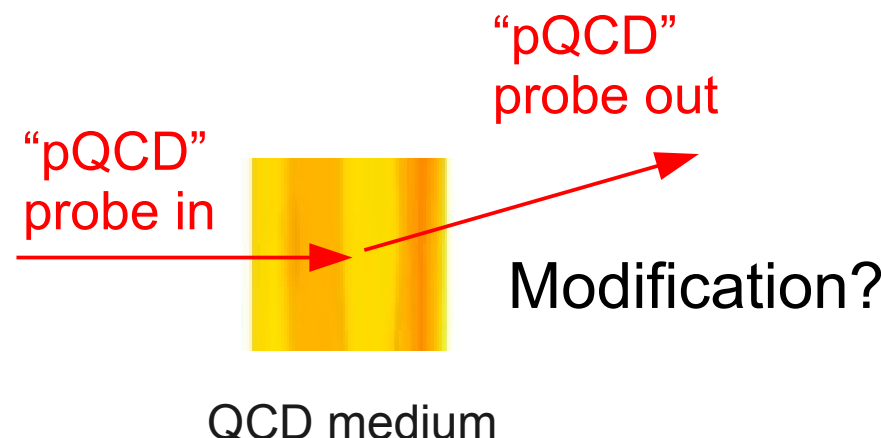
Soft p_T

High p_T

Tomography of QCD matter

18

- Hard (large Q^2) probes of QCD matter:
jets, heavy-quark, $Q\bar{Q}$, γ , W , Z
 - “Self-generated” in the collision at $\tau < 1/Q$ (or $\tau < 1/m$) $< 0.1 \text{ fm}/c$
 - “Tomographic” probes of hottest and densest phase of medium

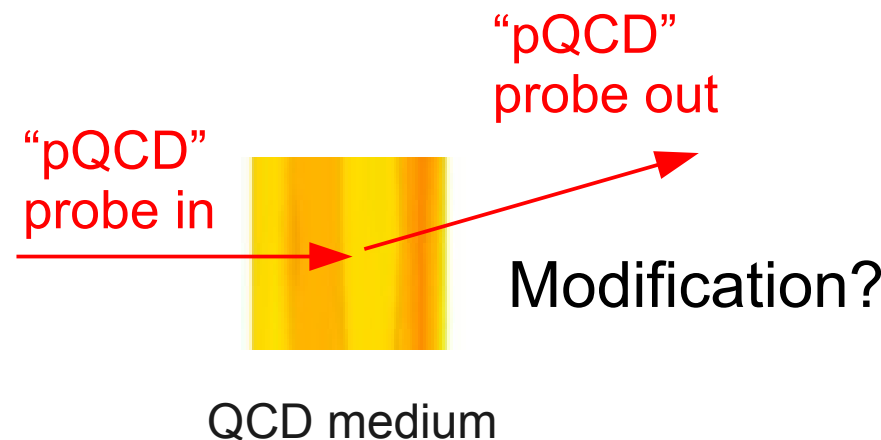


Tomography of QCD matter

19

- Hard (large Q^2) probes of QCD matter: jets, heavy-quark, $Q\bar{Q}$, γ , W , Z

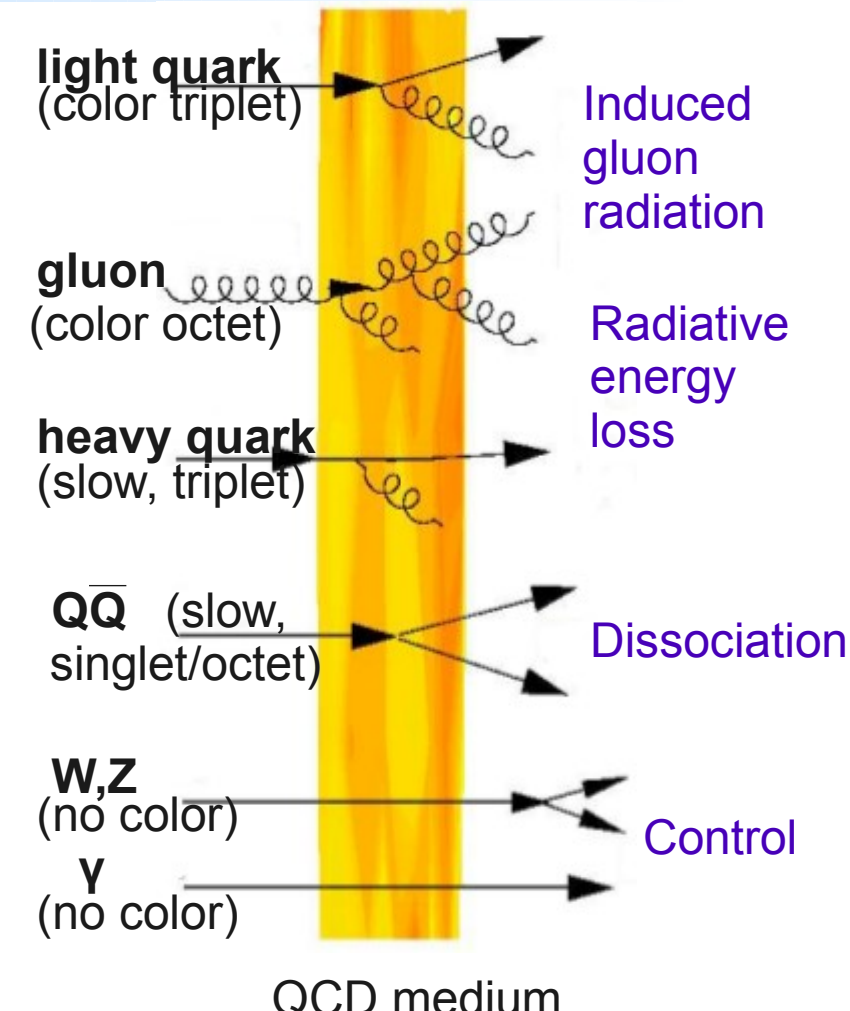
- “Self-generated” in the collision at $\tau < 1/Q$ (or $\tau < 1/m$) $< 0.1 \text{ fm}/c$
- “Tomographic” probes of hottest and densest phase of medium



- Nuclear modification factor

$$R_{AA}(, p_T) = \frac{1}{N_{\text{coll}}} \times \frac{dN_{AA}/dp_T}{dN_{pp}/dp_T} = \frac{dN_{AA}/dp_T}{T_{AA} d\sigma_{pp}}$$

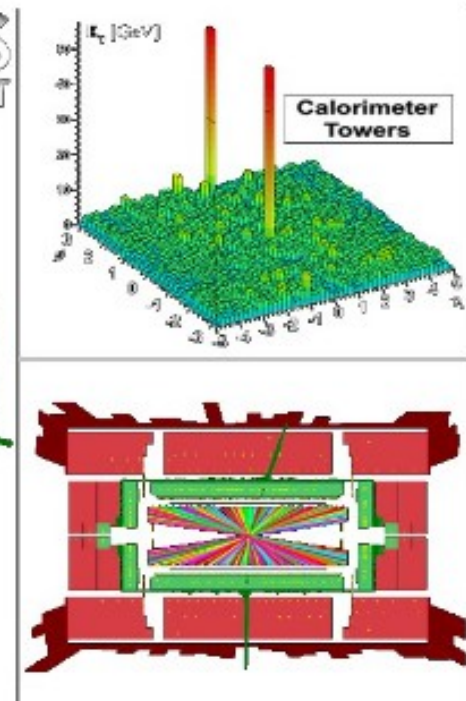
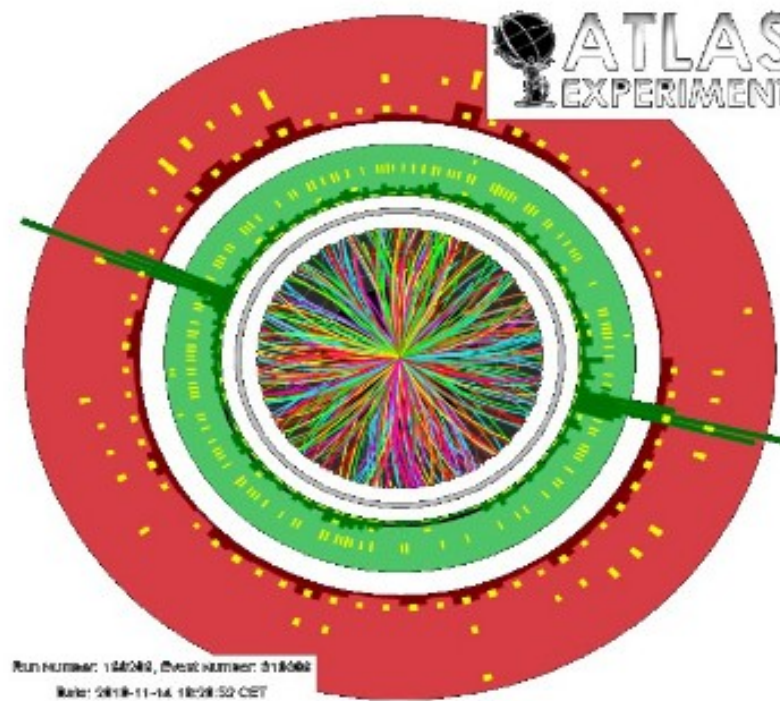
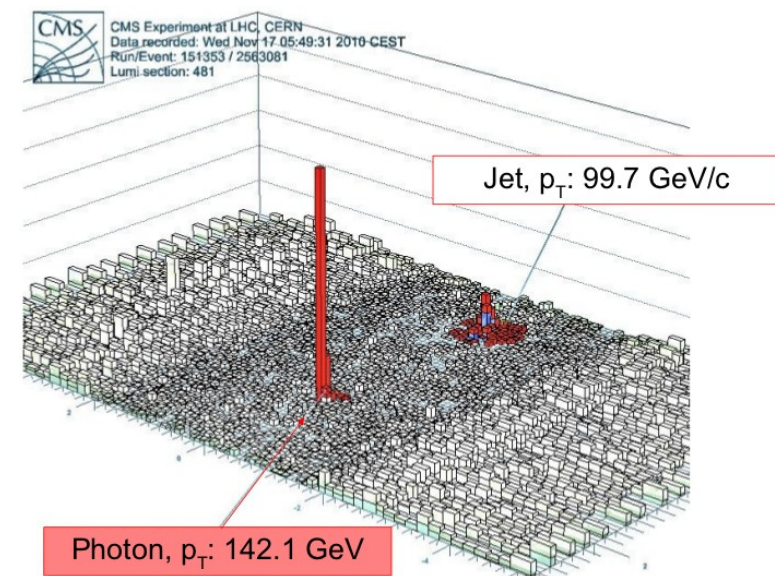
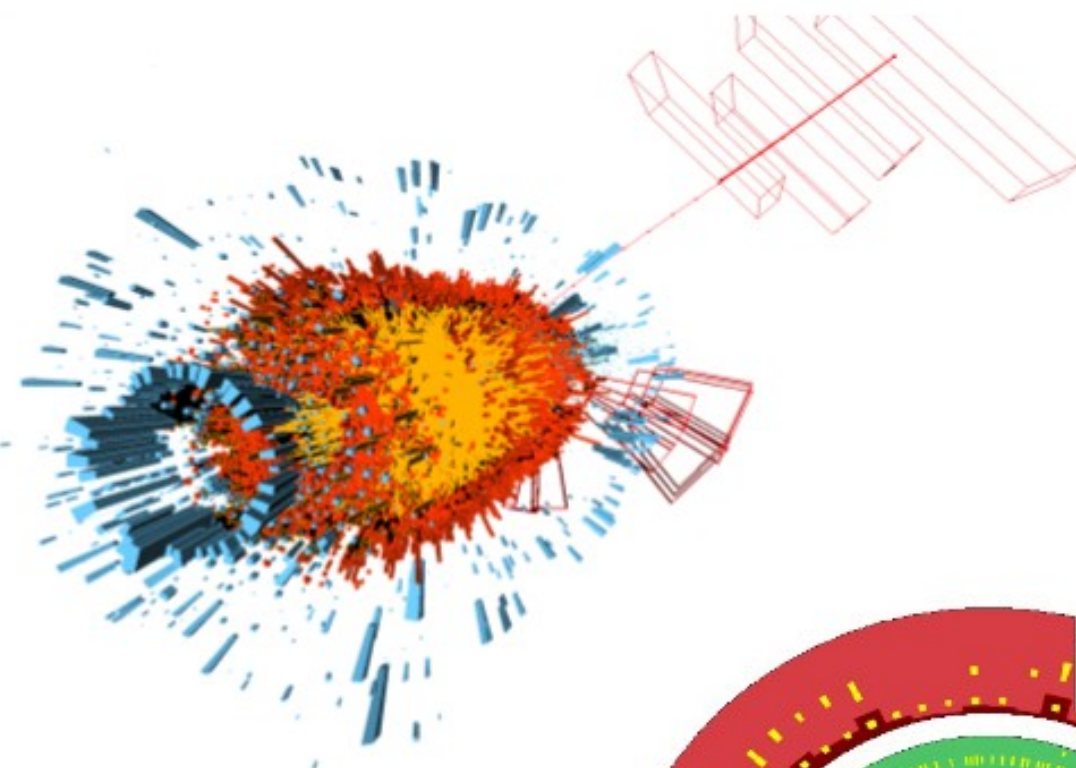
- Quantify change of production rates from expected binary scaling



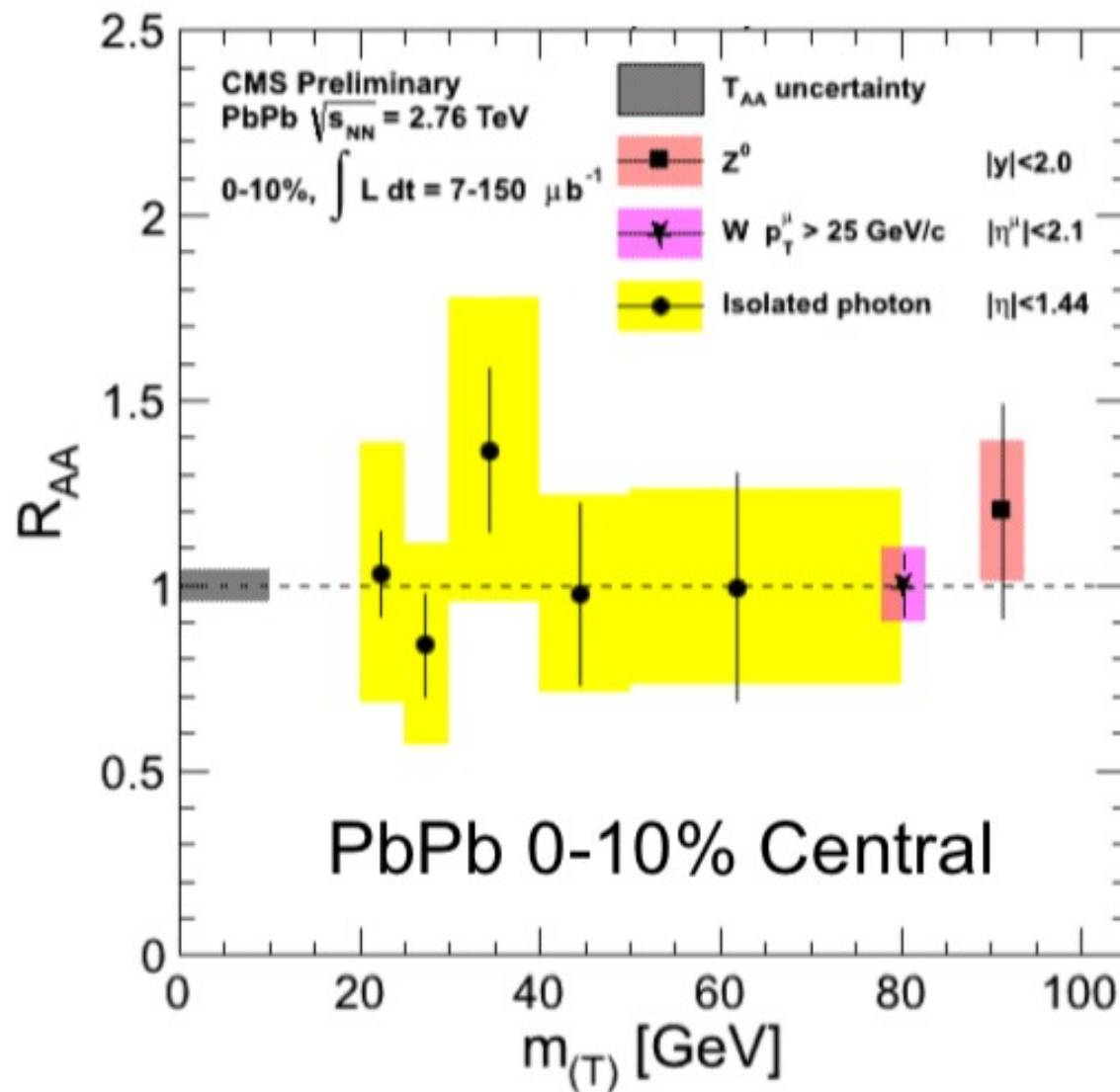
$R_{AA} = 1 \rightarrow$ no deviation from scaling
 $R_{AA} < 1 \rightarrow$ suppression

Isolated γ , W and Z bosons in Pb+Pb

20



Control probes



Isolated γ :

ATLAS, ATLAS-CONF-2012-051
 CMS, PLB 710 (2012) 256

Z boson:

ATLAS, ATLAS-CONF-2012-052
 ATLAS, PLB 697 (2011) 294
 CMS, PRL 106 (2011) 212301

W boson:

ATLAS, ATLAS-CONF-2011-78
 CMS, arXiv:1205.6334

Control probes (isolated γ , Z, W) follow expected scaling ie. $R_{\text{AA}} \sim 1$

Jet quenching

22

Elastic energy loss:

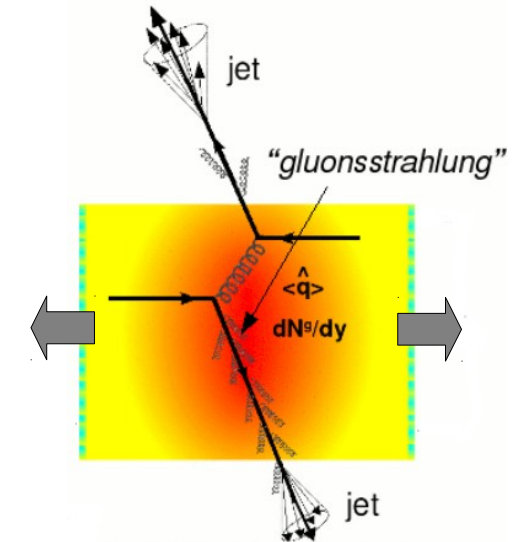
$$\frac{dE}{dx} = -C_2 \hat{e}$$

Radiative energy loss:

$$\frac{dE}{dx} = -C_2 \hat{q} L$$

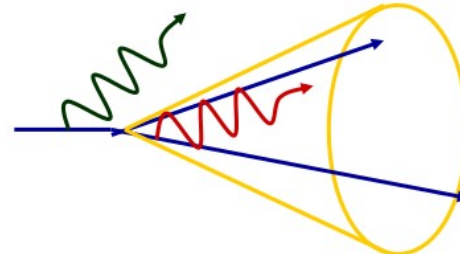
Energy/momentum diffusion tensor:
encodes properties of the medium.

- Induced radiation
 - Increased splitting probability (broadens radiation)
 - Finite quark mass vetos small angle radiation (dead-cone effect)
 - Modified angular pattern due to enhanced incoherence between successive splittings
- Color exchange with medium
 - Modifies color flow in the jet (affects hadronization)
- Modelling dependence
 - Piecewise description
 - Approximations



Search for effects in data:

Out-of-cone radiation (Jet $R_{AA} < 1$)



In-cone radiation
(FF modification)

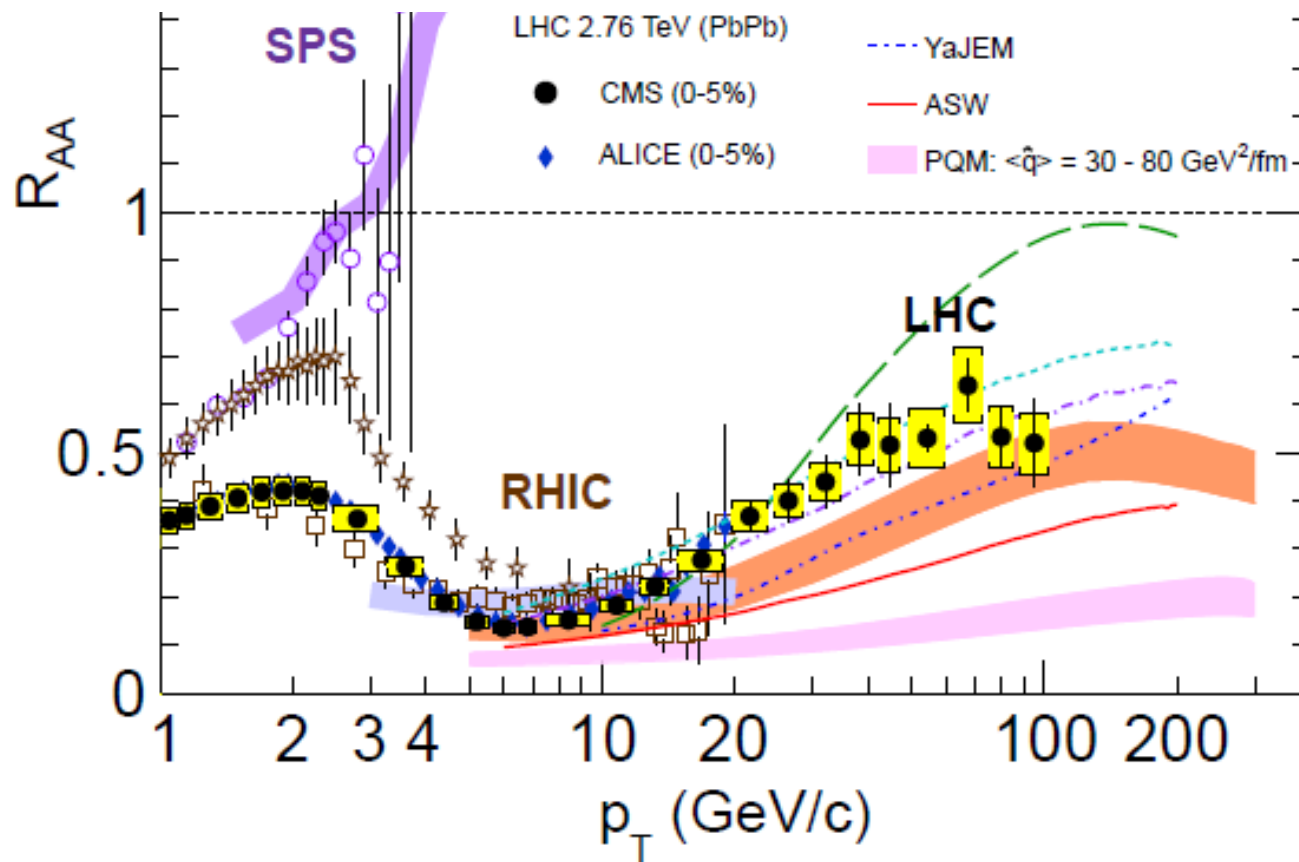
$\Delta E_{\text{loss}}(g) > \Delta E_{\text{loss}}(q) > \Delta E_{\text{loss}}(Q)$

(color factor) (dead-cone effect)

Check $R_{AA}(\pi) < R_{AA}(D) < R_{AA}(B)$

Charged particle suppression

23

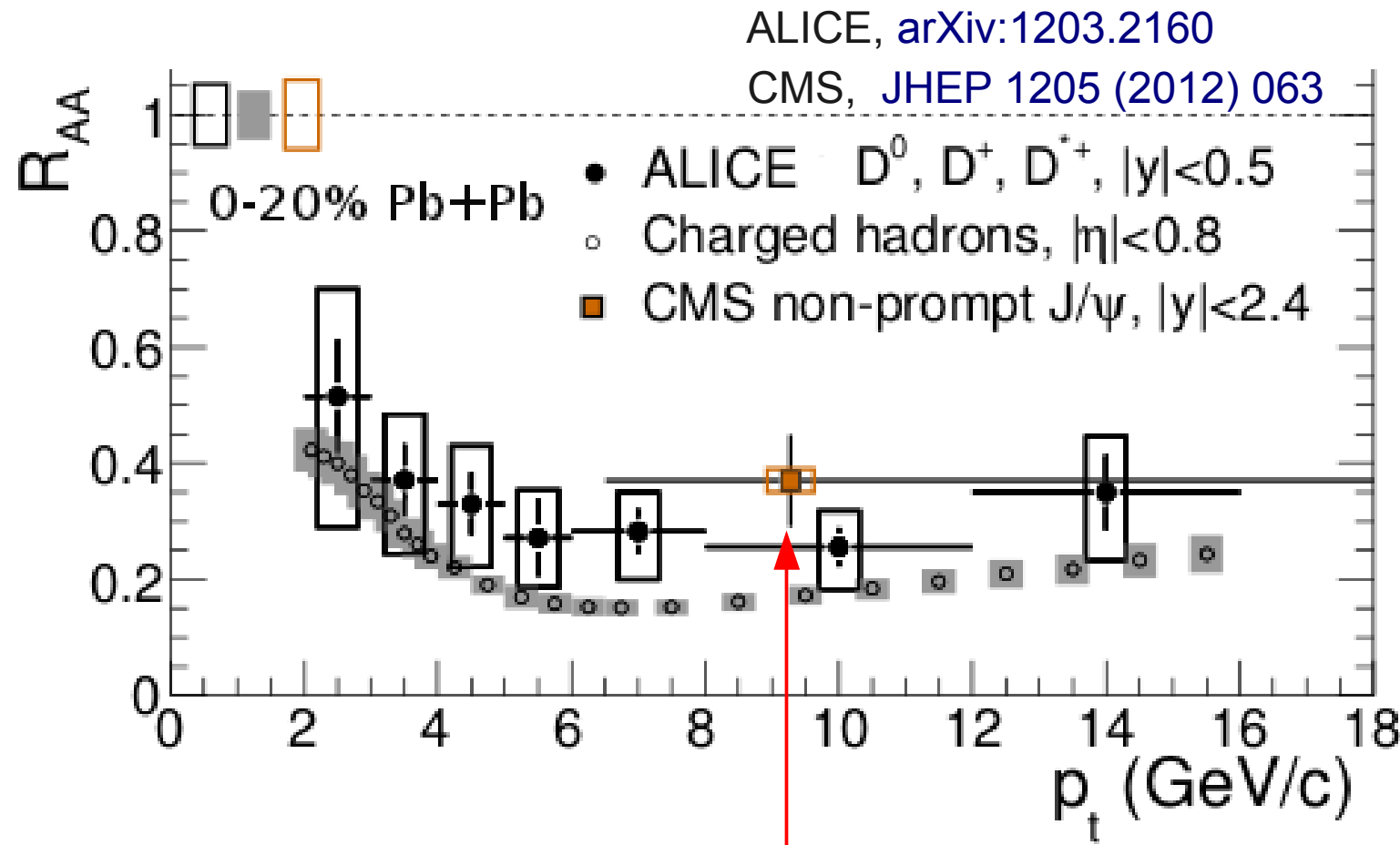


CMS, EPJC 72 (2012) 1945
ALICE, PLB 696 (2011) 30
ATLAS, ATLAS-CONF-2011-079

- Leading hadron suppression up to a factor ~ 7 (at $p_T \sim 7 \text{ GeV}/c$)
 - Slow rise, up to a plateau that may be reached at $p_T > 35 \text{ GeV}/c$
- Strong discrimination power for jet quenching models
 - Test role of initial state with $p+Pb$ run

D and B meson suppression

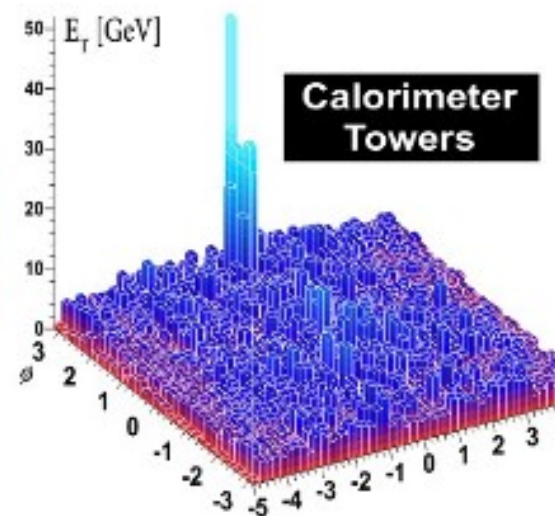
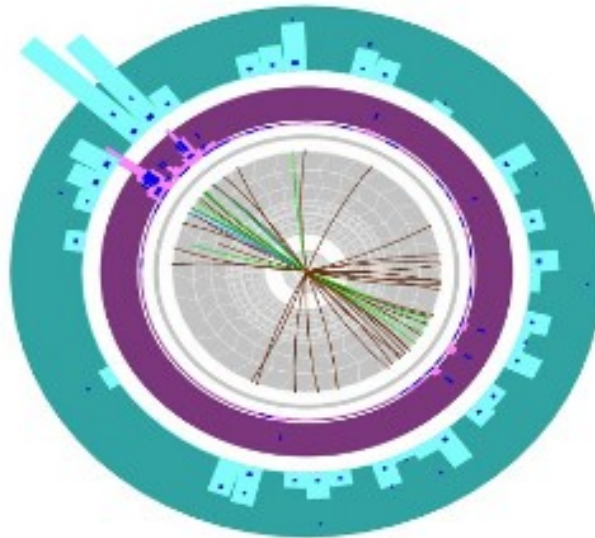
24



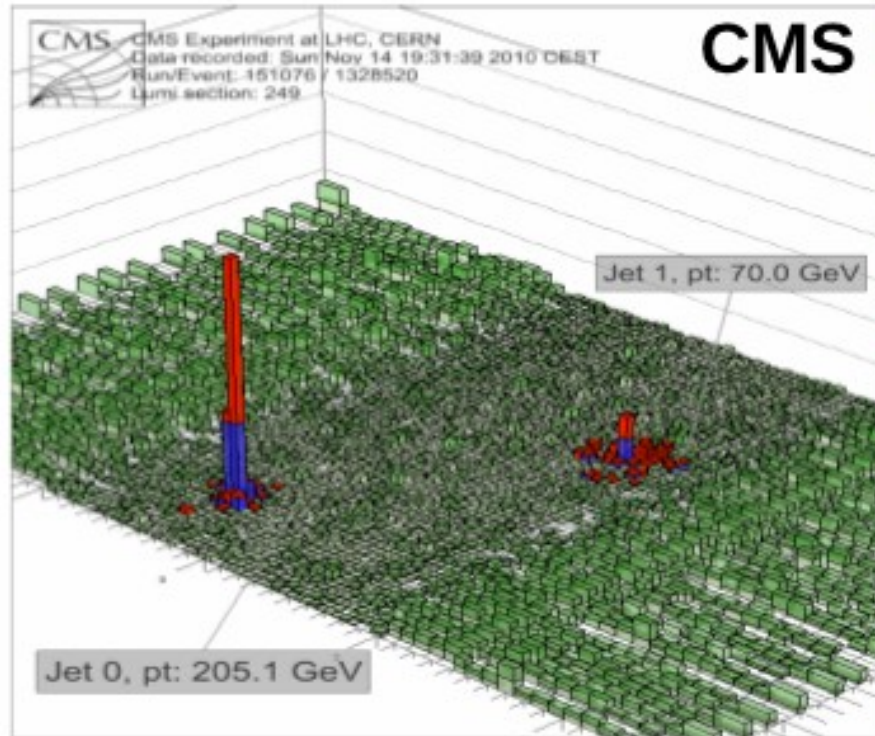
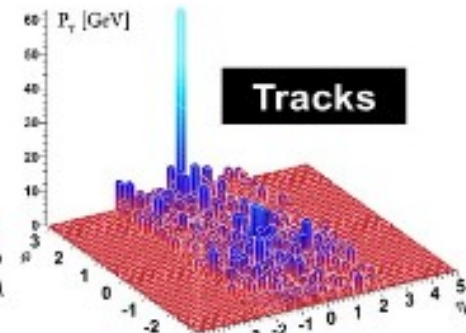
- D-meson suppression factor imposes new constraints on energy loss models (mass & colour charge dependence)
- $R_{AA}(\pi) < R_{AA}(D) < R_{AA}(B)$?
Suppression pattern (within uncertainties) could be compatible with expected energy loss hierarchy

Jet quenching in dijet events

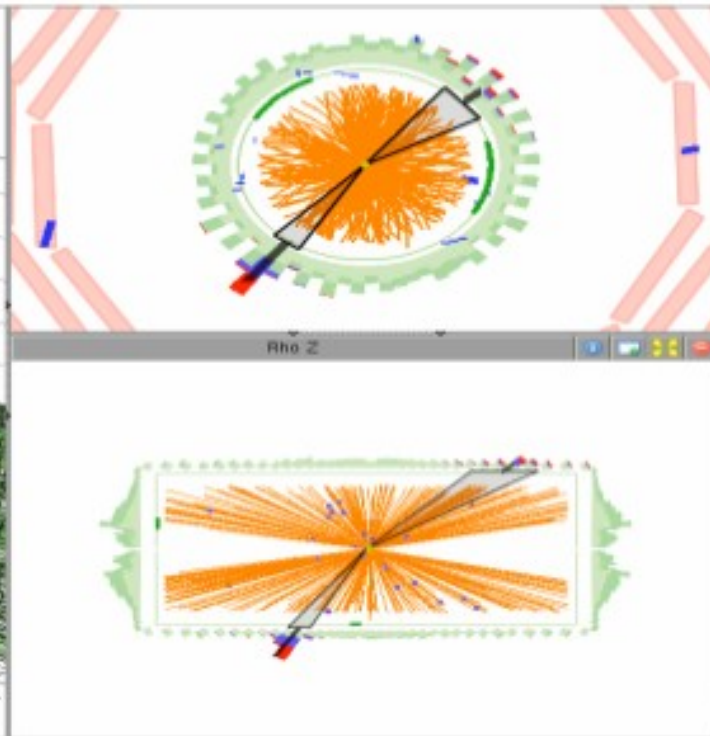
25



ATLAS
Run: 169045
Event: 1914004
Date: 2010-11-12
Time: 04:11:44 CET



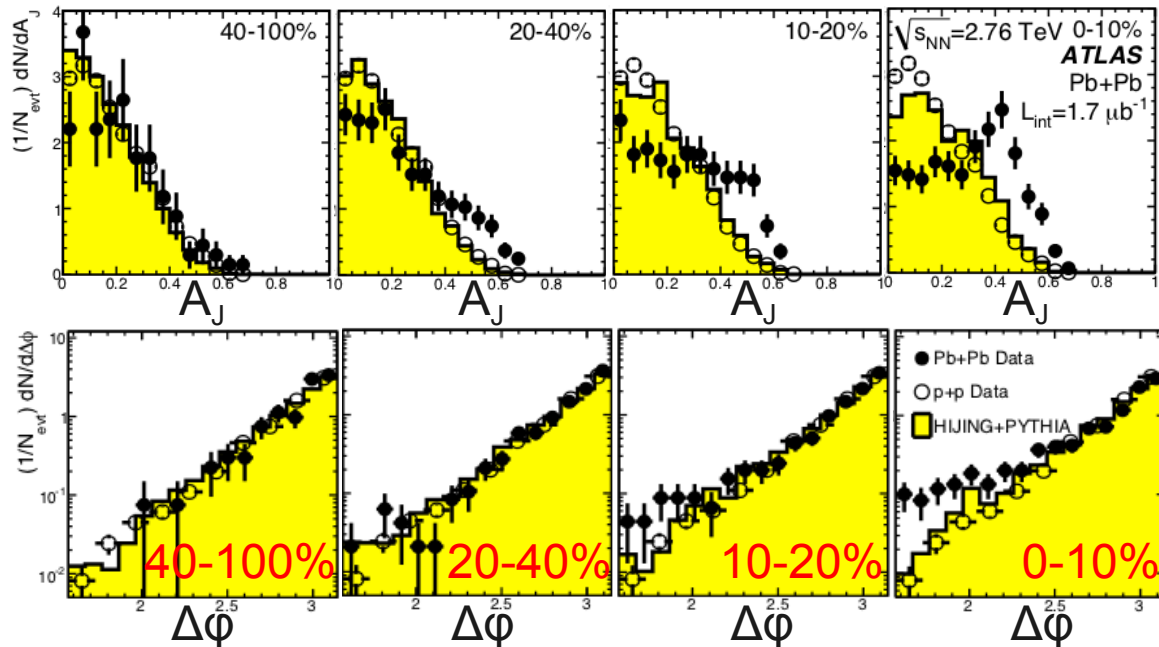
CMS



Dijet momentum imbalance

26

Dijet momentum imbalance: $A_J = (p_{T,1} - p_{T,2}) / (p_{T,1} + p_{T,2})$ ($p_{T,1} > 100$, $p_{T,2} > 25$ GeV/c)

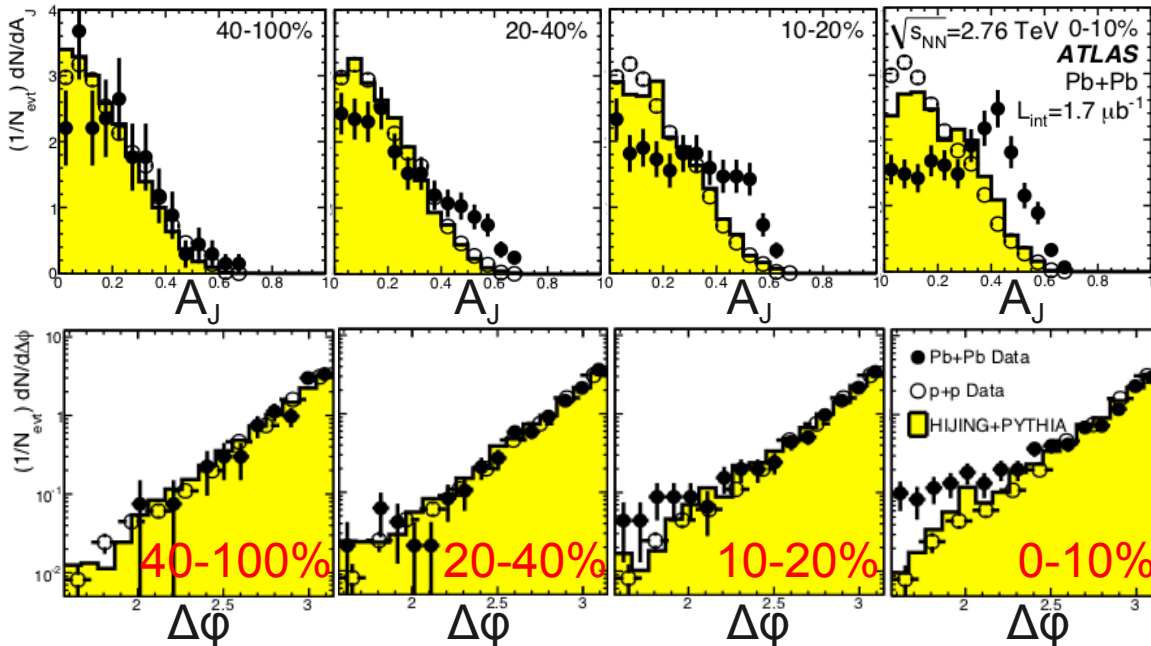


Larger momentum imbalance wrt to MC reference.
Difference increases with increasing centrality.
But no (very little) increasing azimuthal decorrelation.

ATLAS, PRL 105 (2010) 252303
CMS, PRC84 (2011) 024906

Dijet momentum imbalance

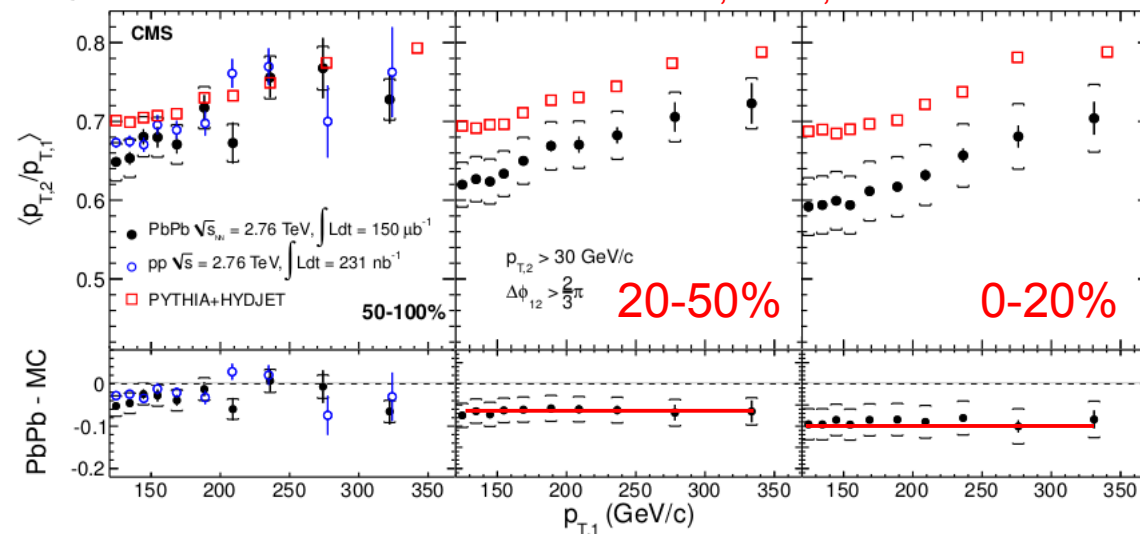
Dijet momentum imbalance: $A_J = (p_{T,1} - p_{T,2}) / (p_{T,1} + p_{T,2})$ ($p_{T,1} > 100$, $p_{T,2} > 25$ GeV/c)



Larger momentum imbalance wrt to MC reference.
Difference increases with increasing centrality.
But no (very little) increasing azimuthal decorrelation.

ATLAS, PRL 105 (2010) 252303
CMS, PRC84 (2011) 024906

Dijet momentum ratio: $p_{T,2}/p_{T,1}$ vs leading jet $p_{T,1}$

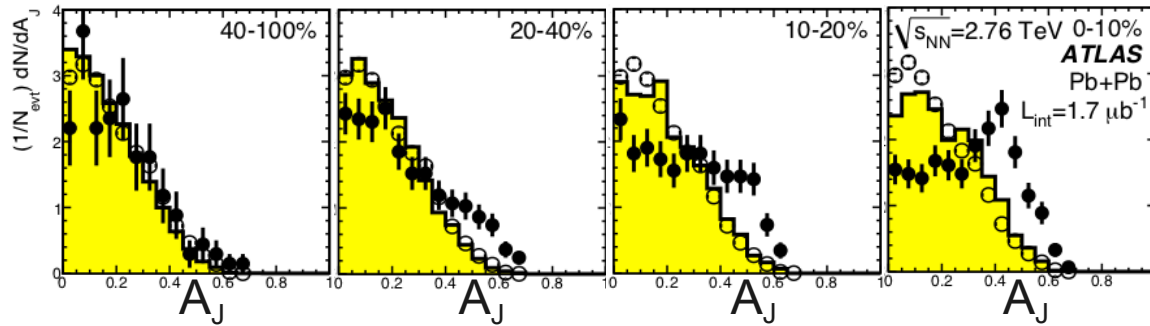


Even ~350 GeV/c jets are quenched!
Fraction of energy lost constant up to ~350 GeV/c.

CMS, PLB 712 (2012) 176

Dijet momentum imbalance

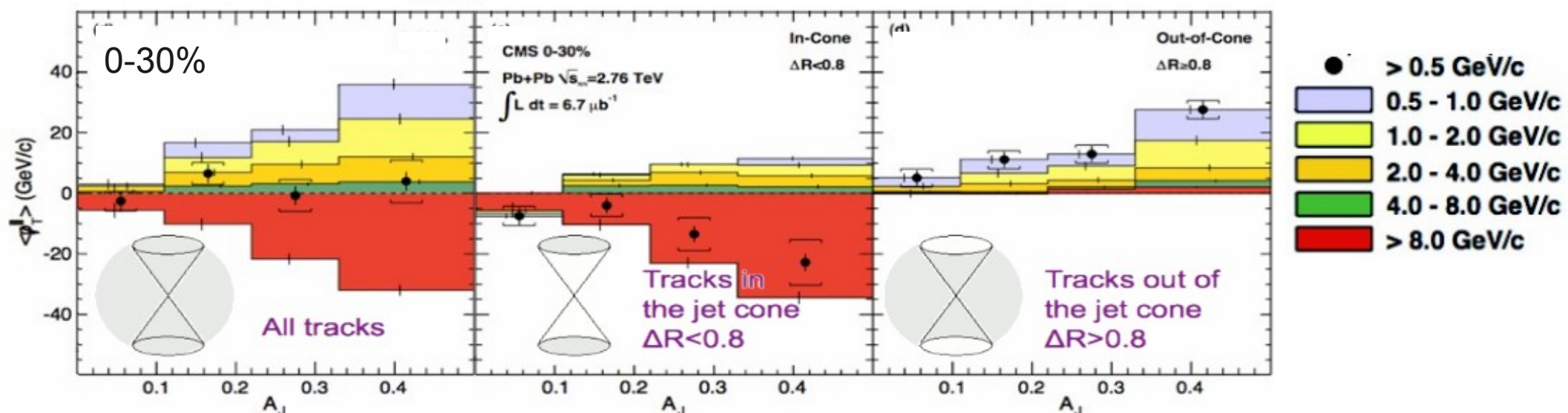
Dijet momentum asymmetry: $A_J = (p_{T,1} - p_{T,2})/(p_{T,1} + p_{T,2})$



ATLAS, PRL 105 (2010) 252303
CMS, PRC84 (2011) 024906

Lost energy emitted at low p_T ($< 4 \text{ GeV}/c$) outside jet cone ($R > 0.8$)

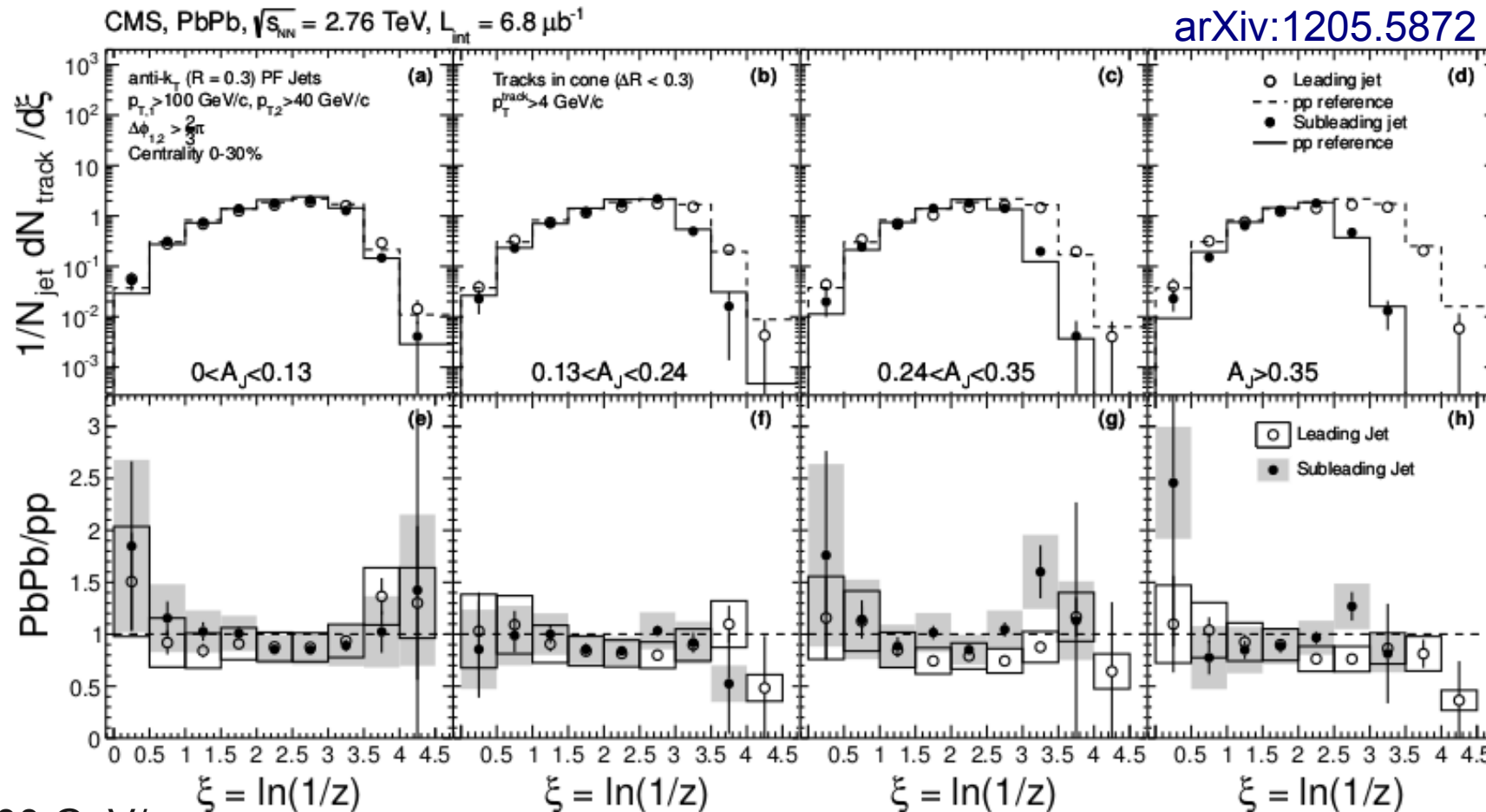
$$p_T^{\parallel} = \sum_{\text{Tracks}} -p_T^{\text{Track}} \cos(\phi_{\text{Track}} - \phi_{\text{Leading Jet}})$$



Jet fragmentation function

29

Fragmentation functions constructed using tracks with $p_T > 4 \text{ GeV}/c$ in $R < 0.3$ and the reconstructed (quenched) jet energy



$P_{T1} > 100 \text{ GeV}/c$

$P_{T2} > 40 \text{ GeV}/c$

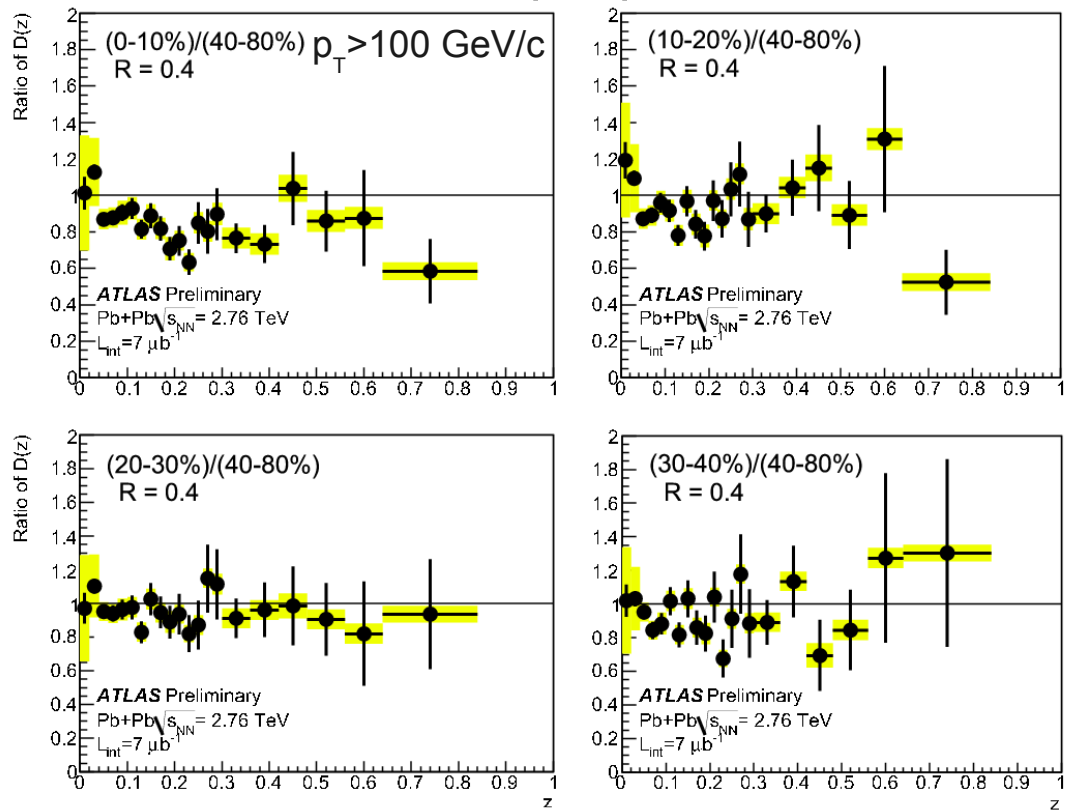
$\Delta\Phi_{12} > 2/3\pi$

Track $p_T > 4 \text{ GeV}/c$

Leading and sub-leading jet in Pb+Pb fragment
like jets of corresponding energy in pp

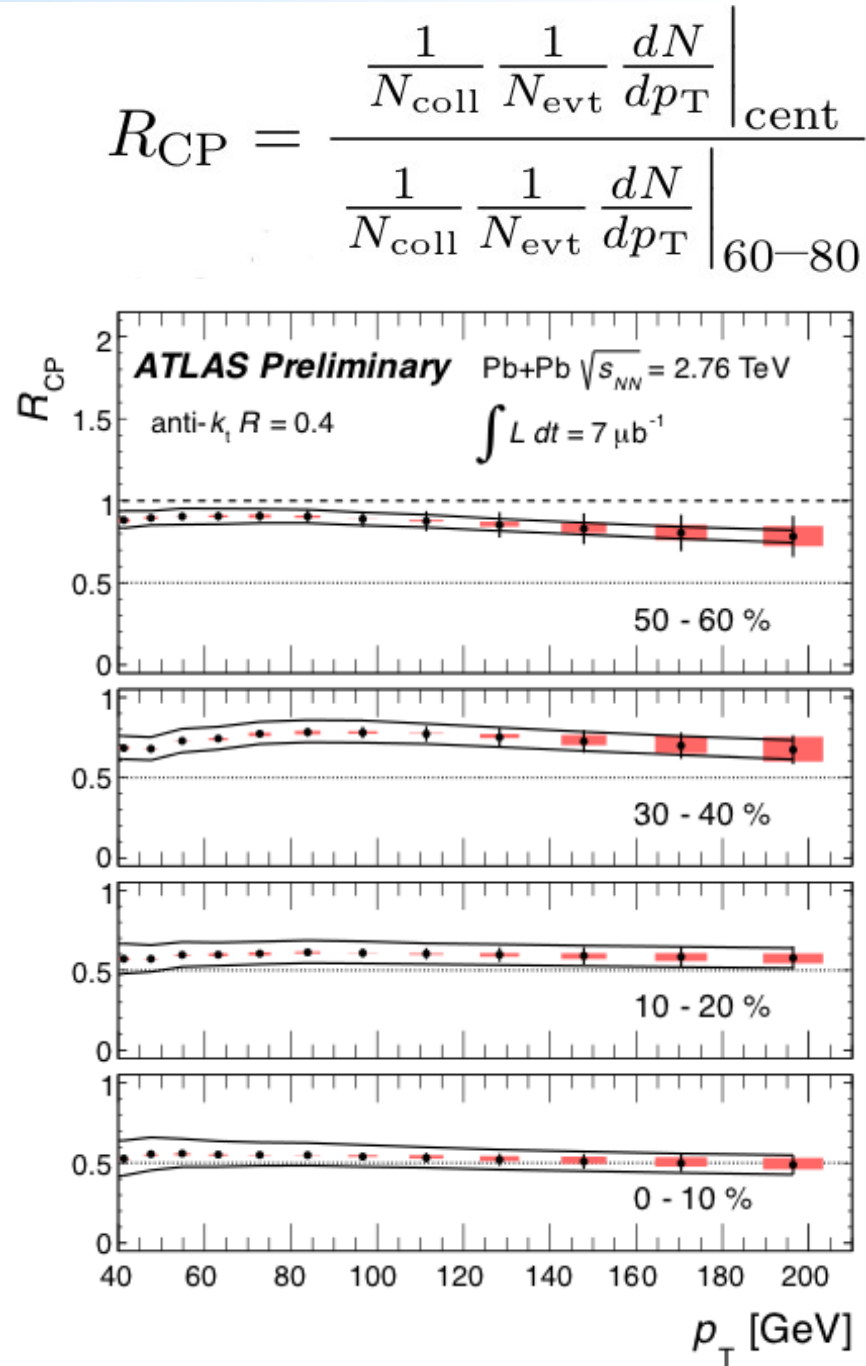
Inclusive jet R_{cp}

Ratio of fragmentation function
in central over peripheral events



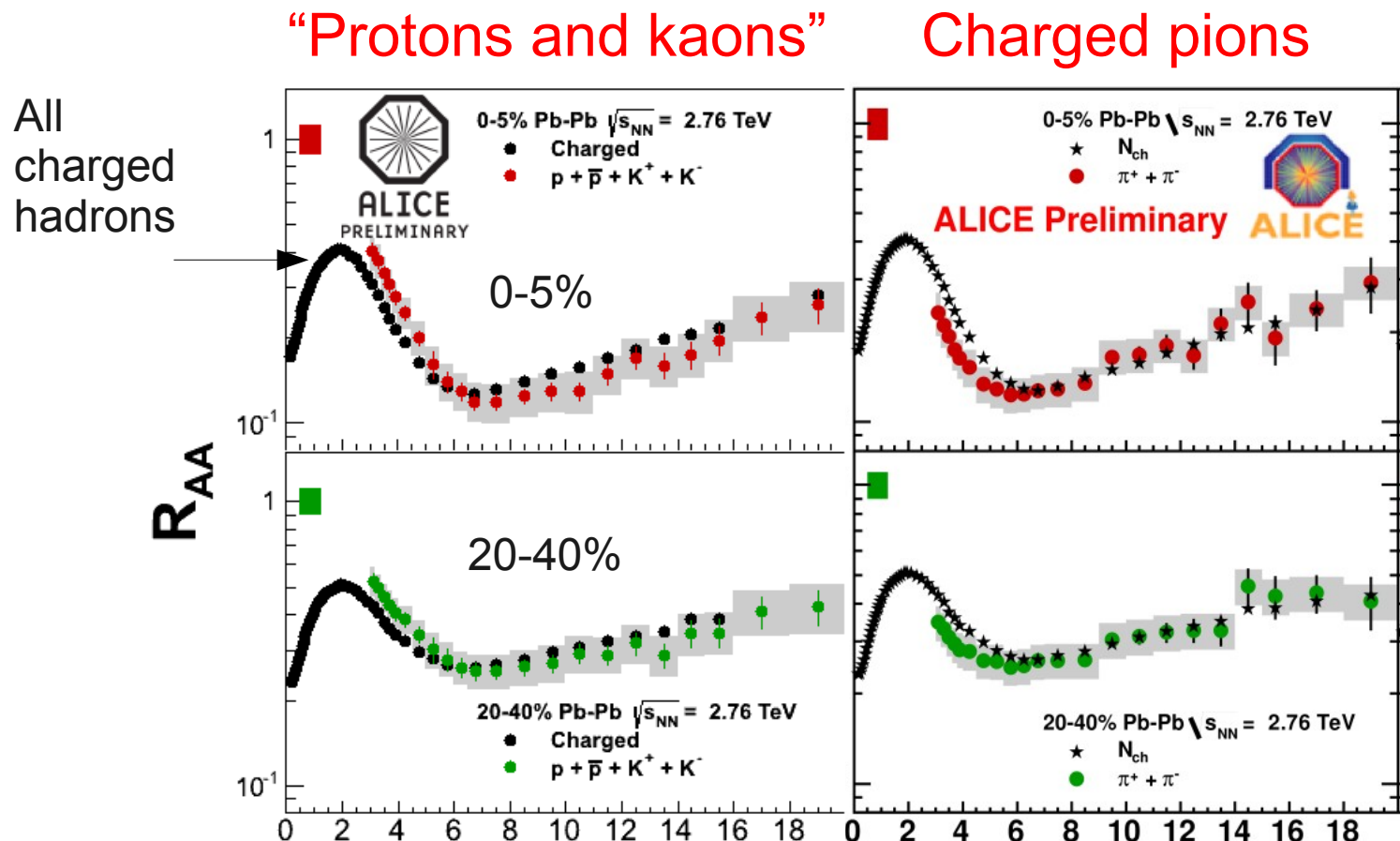
ATLAS-CONF-2011-075

No strong modification of the
fragmentation function between
peripheral and central events.
Jet R_{cp} independent on energy.



Identified particle R_{AA} at high p_T

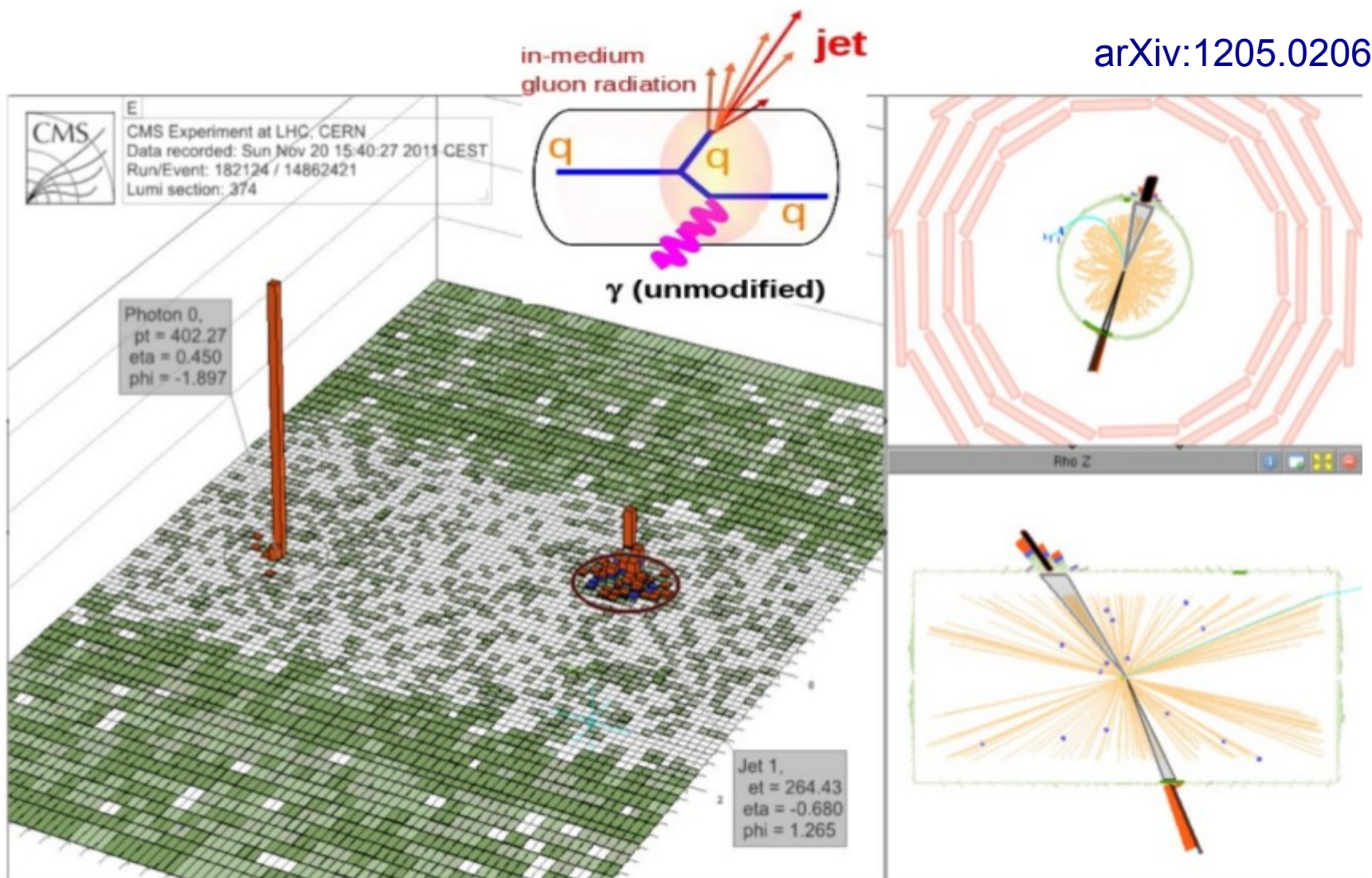
31



Little room for in-medium modification at high p_T

Jet quenching in γ -jet events

32



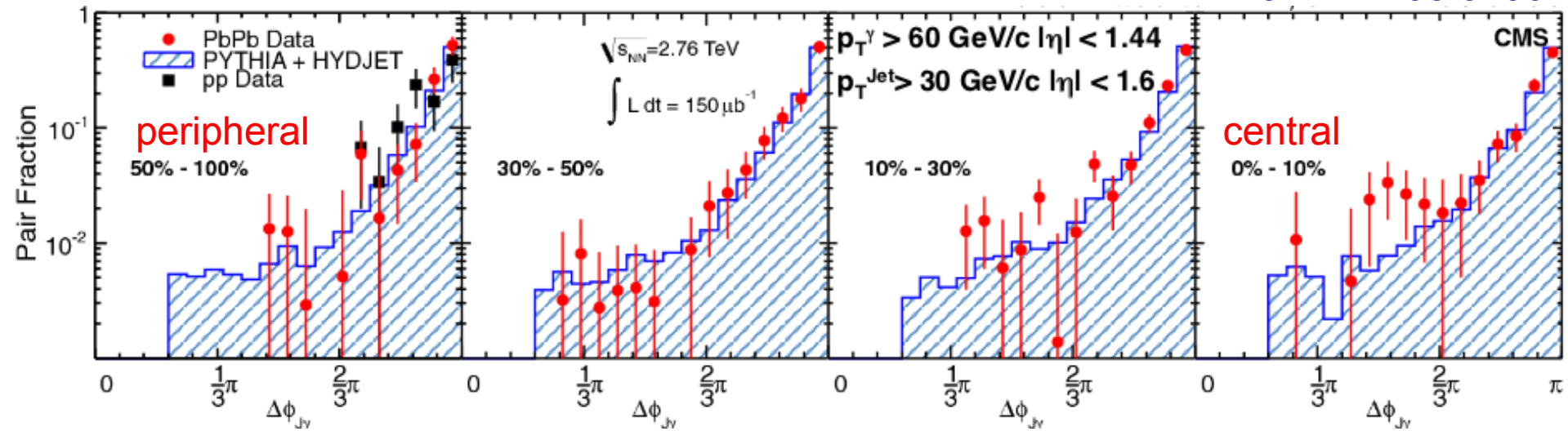
Photon $p_T > 60$ GeV/c

Jet $p_T > 30$ GeV/c

γ -jet azimuthal correlation

33

arXiv:1205.0206

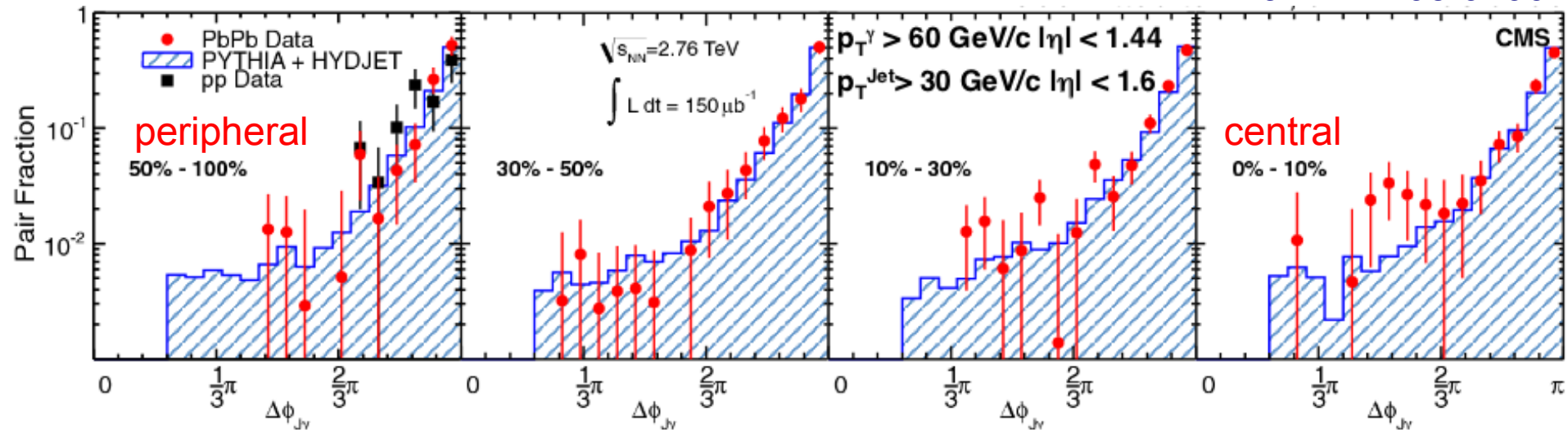


- Azimuthal correlation consistent with pp and MC (PYTHIA+HYDJET)

γ -jet azimuthal correlation

34

arXiv:1205.0206



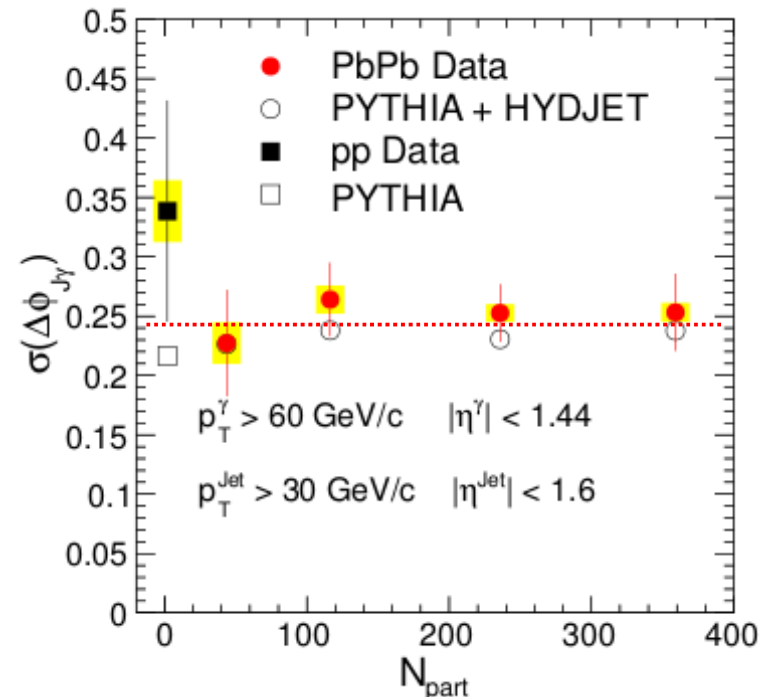
- Azimuthal correlation consistent with pp and MC (PYTHIA+HYDJET)

- Angular width parametrized with

$$\frac{1}{N_{J\gamma}} \frac{dN_{J\gamma}}{d\Delta\phi_{J\gamma}} = \frac{e^{(\Delta\phi-\pi)/\sigma}}{(1-e^{-\pi/\sigma})\sigma}$$

constant vs centrality

- Quenched jet is back-to-back to γ : Energy transfer not via one single hard gluon radiation

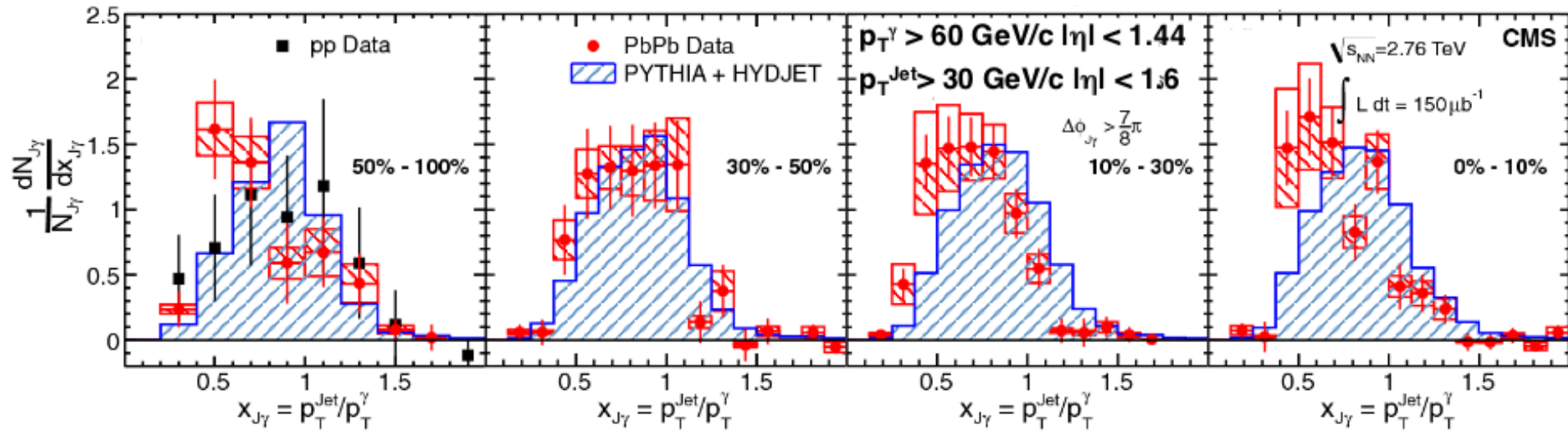


γ -jet momentum imbalance

35

Momentum ratio distribution

arXiv:1205.0206



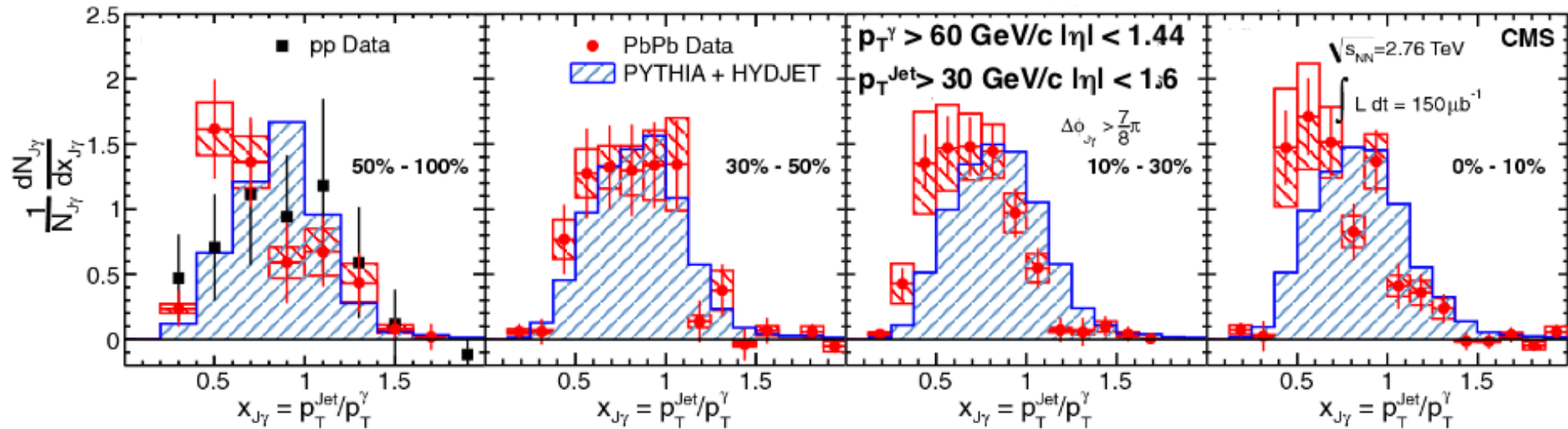
Increasing centrality →

γ -jet momentum imbalance

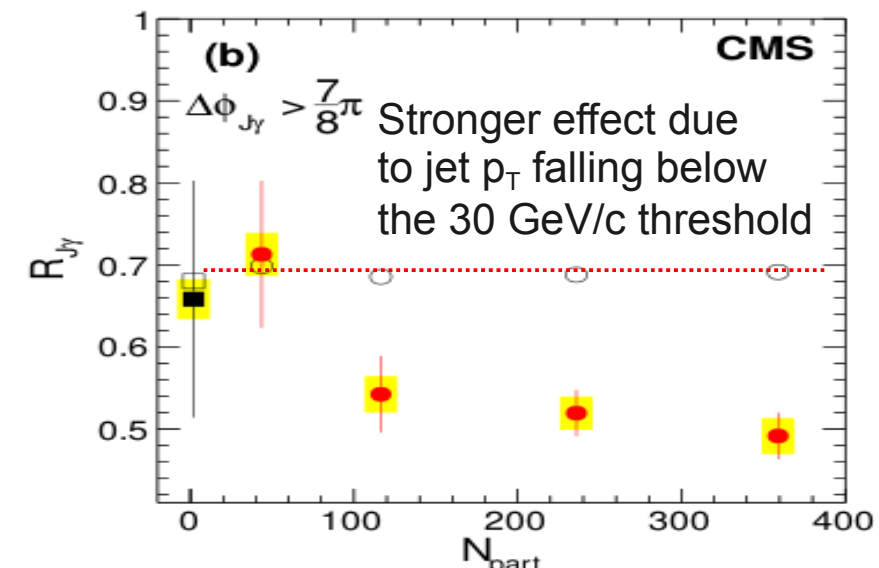
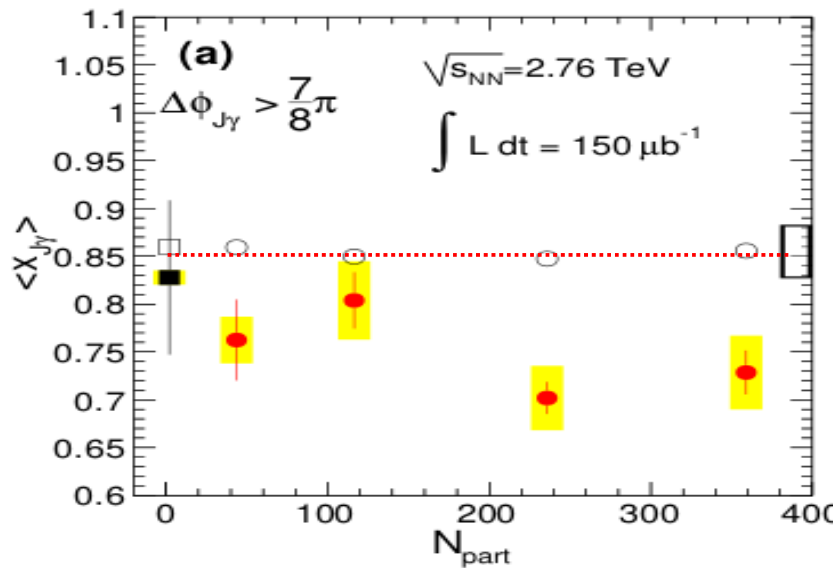
36

Momentum ratio distribution

arXiv:1205.0206



Momentum ratio ($x_{J\gamma}$) and fraction of γ -jet associations ($R_{J\gamma}$) decrease significantly with centrality compared to pp or MC



- The LHC is ideal for studying the QGP
 - Hotter, larger, longer lifetime, hard probes
 - QGP has similar “perfect liquid” properties as at RHIC
 - Proton/pion ratio to be understood
- The LHC is a “hard probes” machine
 - There has been a burst of new data and observables.
 - And there is still quite a lot of data to analyze.
 - Should attempt to describe all aspects (incl. details) in common model.
 - Upcoming p+Pb run in fall 2012 will reduce some of the uncertainties due to initial state effects

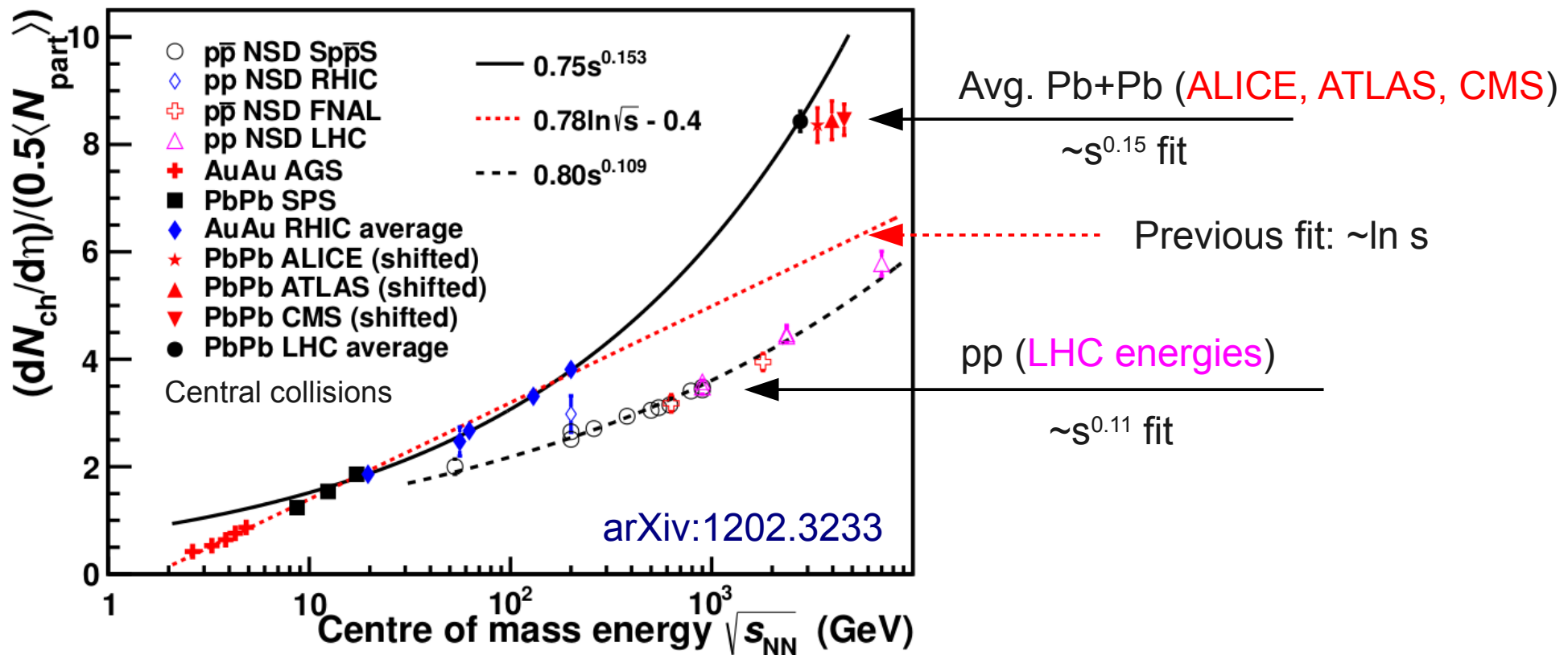
Special thanks to ALICE, ATLAS and CMS collaborations for their material, and to the LHC for an excellent performance.

Extra slides

38

Energy dependence of $dN/d\eta$

39

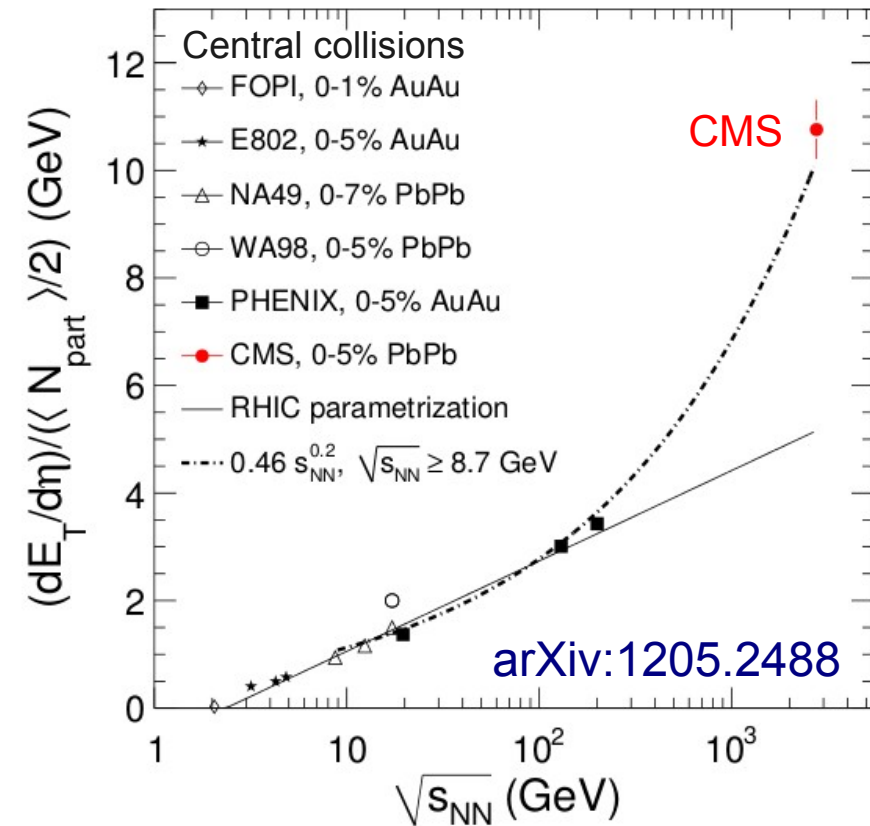
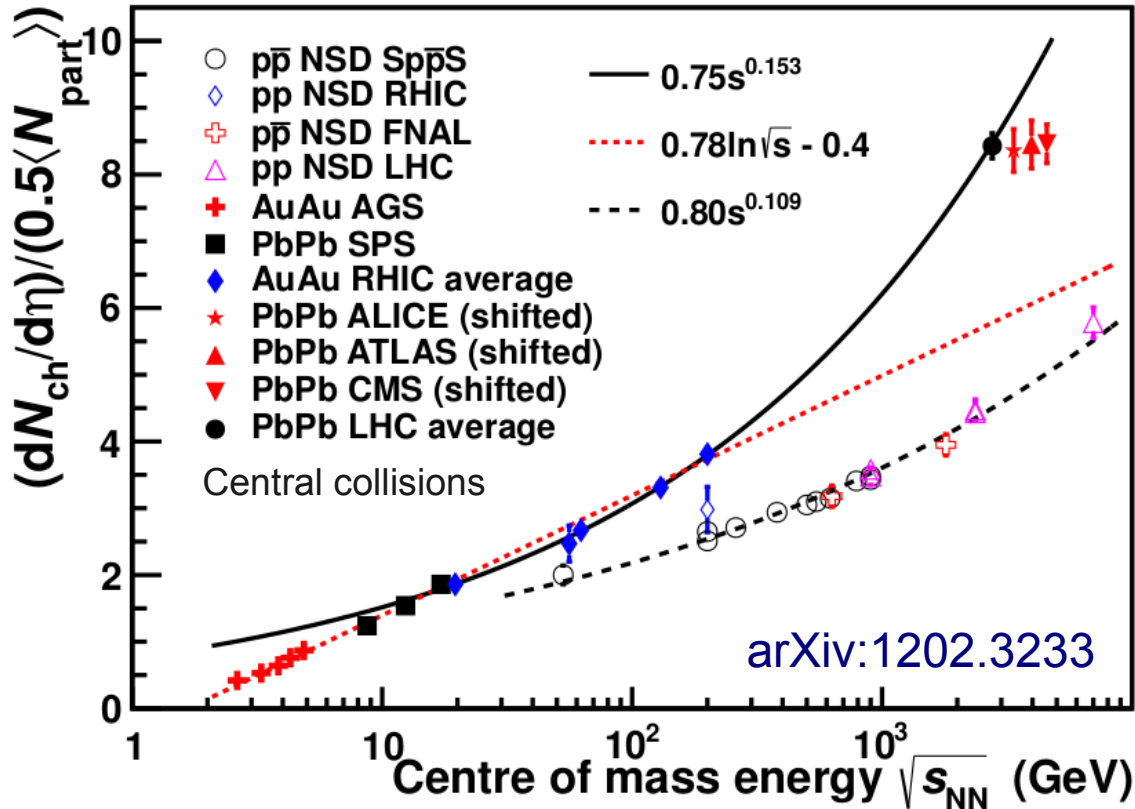


Stronger rise with center-of-mass energy in AA wrt to pp, and wrt to extrapolations from lower energies
 $(dN_{ch}/d\eta)_{LHC} \approx 1600 \sim 2 \times dN_{ch}/d\eta_{RHIC})$

ALICE, PRL 106 (2011) 032301
 CMS, JHEP 1108 (2011) 141
 ATLAS, PLB 710 (2012) 363

Energy dependence of $dN/d\eta$ and $dE_T/d\eta$

40



Stronger rise with center-of-mass energy in AA wrt to pp, and wrt to extrapolations from lower energies
 $(dN_{ch}/d\eta)_{LHC} \approx 1600 \sim 2 \times dN_{ch}/d\eta_{RHIC})$

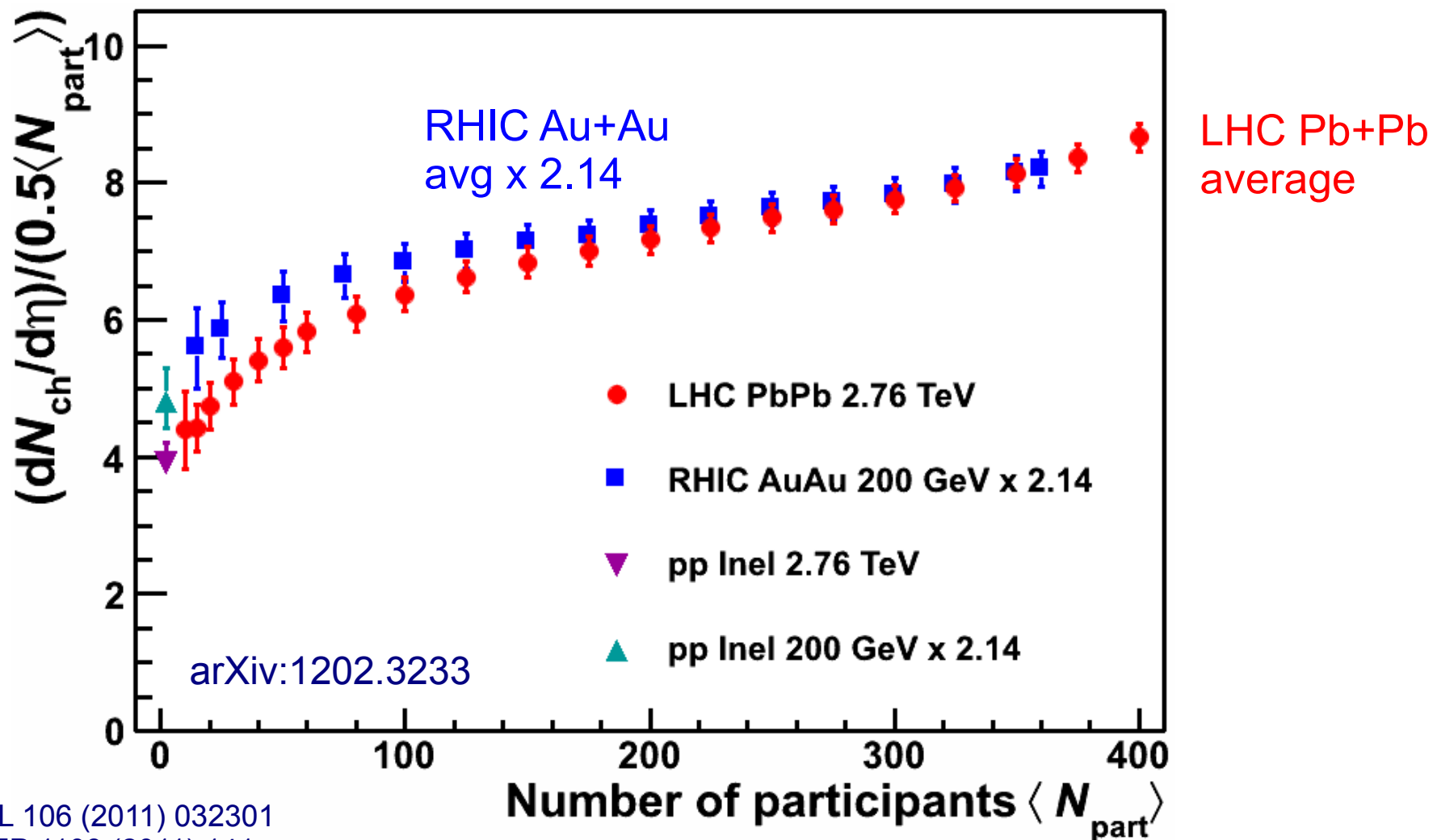
$$\epsilon(\tau) = \frac{dE_T/d\eta}{\pi R^2 \tau} \approx 3/2 \langle m_T \rangle \frac{dN_{ch}/d\eta}{\pi R^2 \tau}$$

$\tau \epsilon_{LHC} \simeq 2.5 \times \tau \epsilon_{RHIC}$

Initial energy density at LHC (as at RHIC) is well above $\varepsilon_c \approx 0.5$ GeV/fm³

Centrality dependence of $dN/d\eta$

41

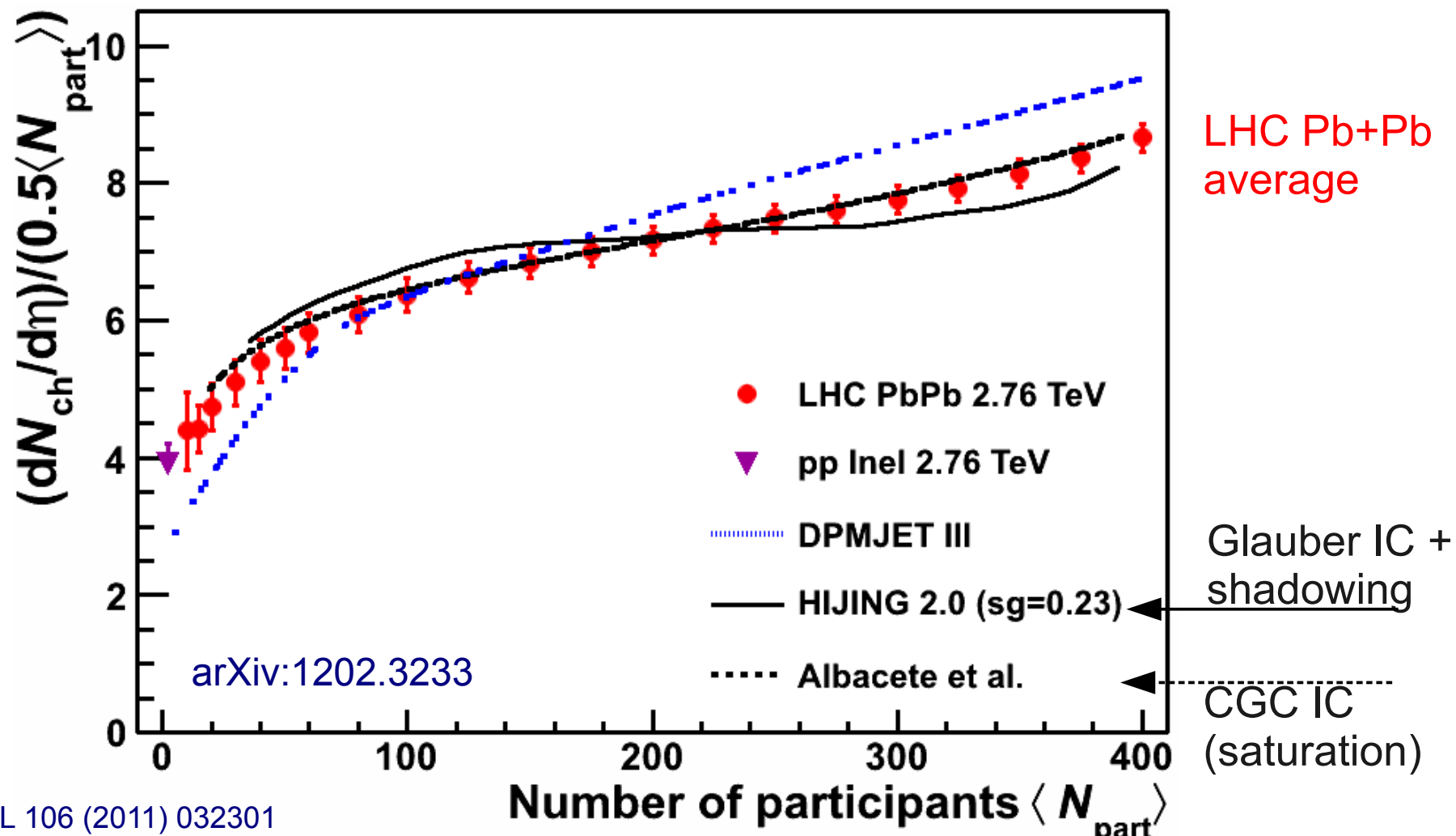


ALICE, PRL 106 (2011) 032301
CMS, JHEP 1108 (2011) 141
ATLAS, PLB 710 (2012) 363

Centrality dependence is strikingly similar to RHIC.
This actually holds all the way down to 19.6 GeV (not shown)

Centrality dependence of $dN/d\eta$

42

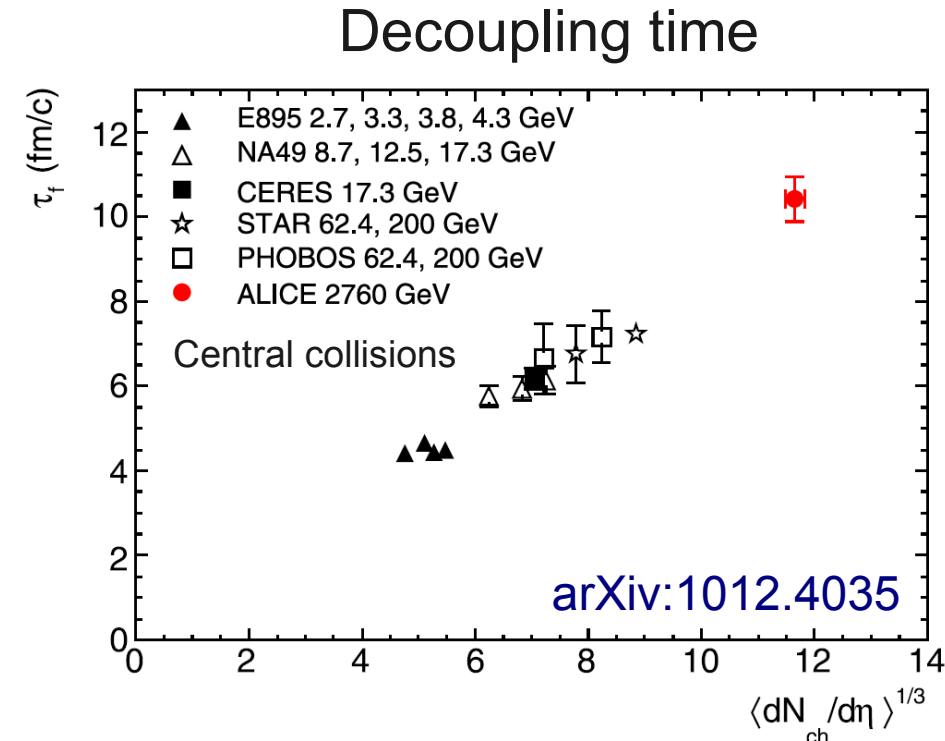
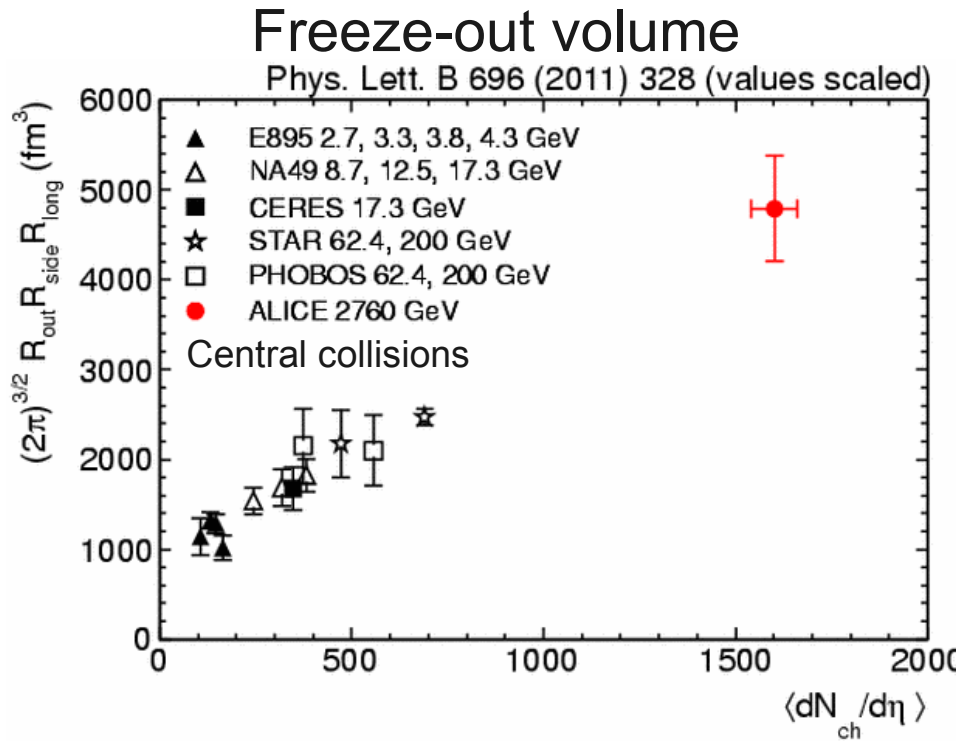


ALICE, PRL 106 (2011) 032301
 CMS, JHEP 1108 (2011) 141
 ATLAS, PLB 710 (2012) 363

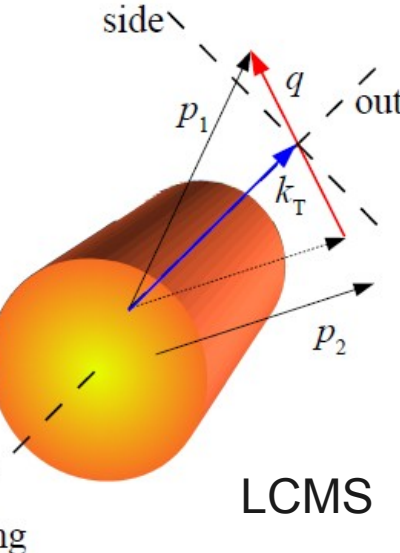
Two-component models need to incorporate strong nuclear modification. Models based on Glauber and CGC initial conditions can describe the data.

Space-time evolution of the system

43

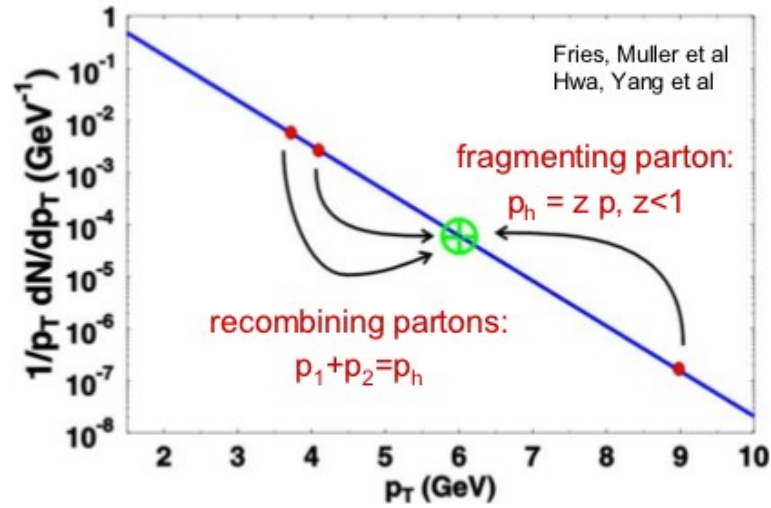
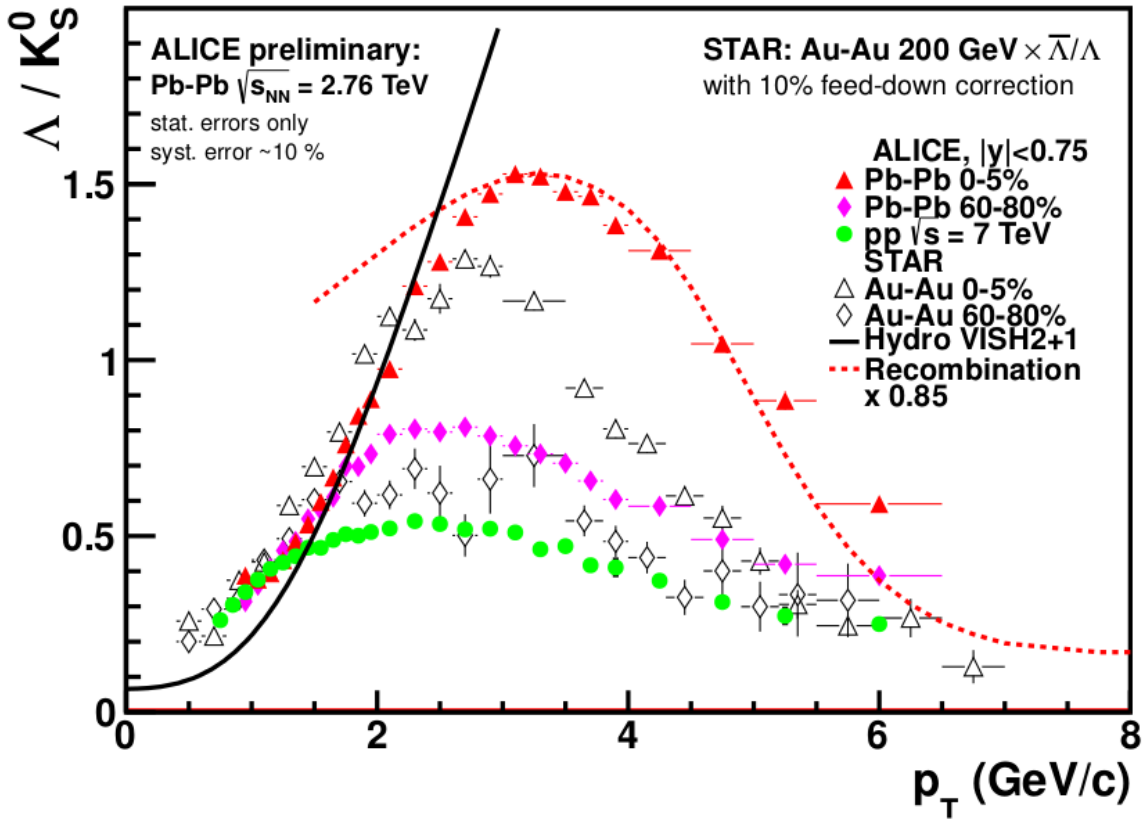


- Use interferometry of identical particles (HBT)
 - Obtain HBT radii of spherical source in 3 orthogonal directions (R_{long} , R_{side} and R_{out})
- Compared to RHIC
 - Freeze-out volume: $V_{\text{LHC}} \approx 5000 \text{ fm}^3 \sim 2 \times V_{\text{RHIC}} > 6 V_{\text{Pb}}$
 - Decoupling time: $\tau_f(\text{LHC}) \approx 10-11 \text{ fm/c} \sim 1.4 \times \tau_f(\text{RHIC})$



Intermediate p_T region

44

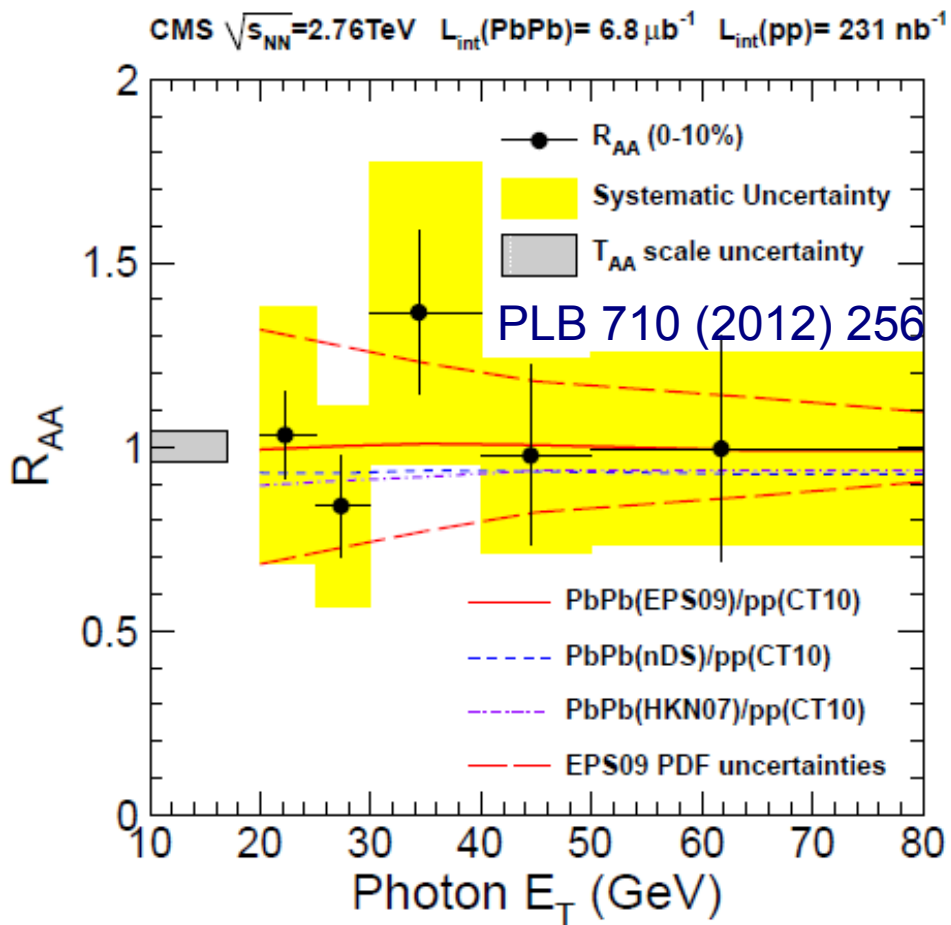
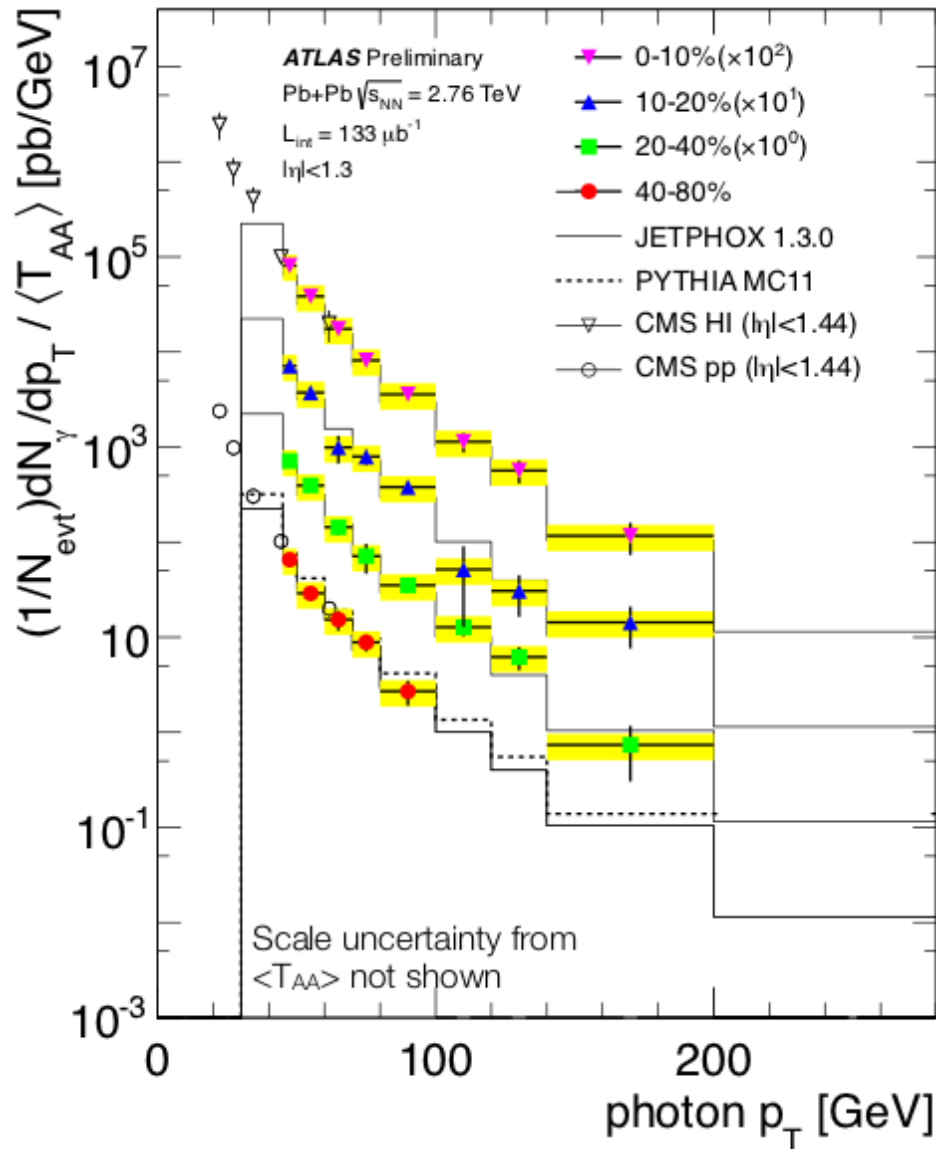


Intermediate region dominated by soft-hard interactions.
Recombination (coalescence) could be at work with
consequences on spectra (but also on v_2).

Control probe: Isolated photons

45

HP12, ATLAS-CONF-2012-051

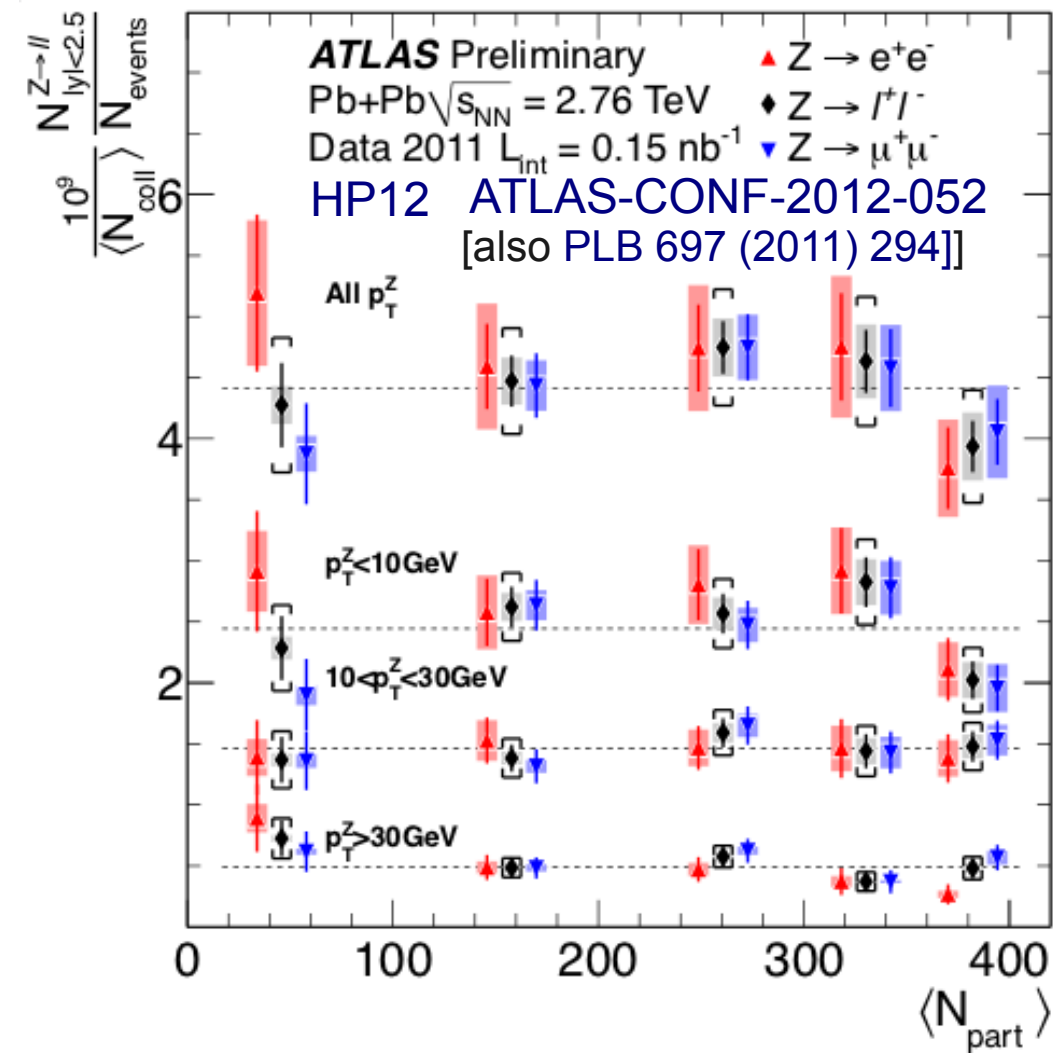
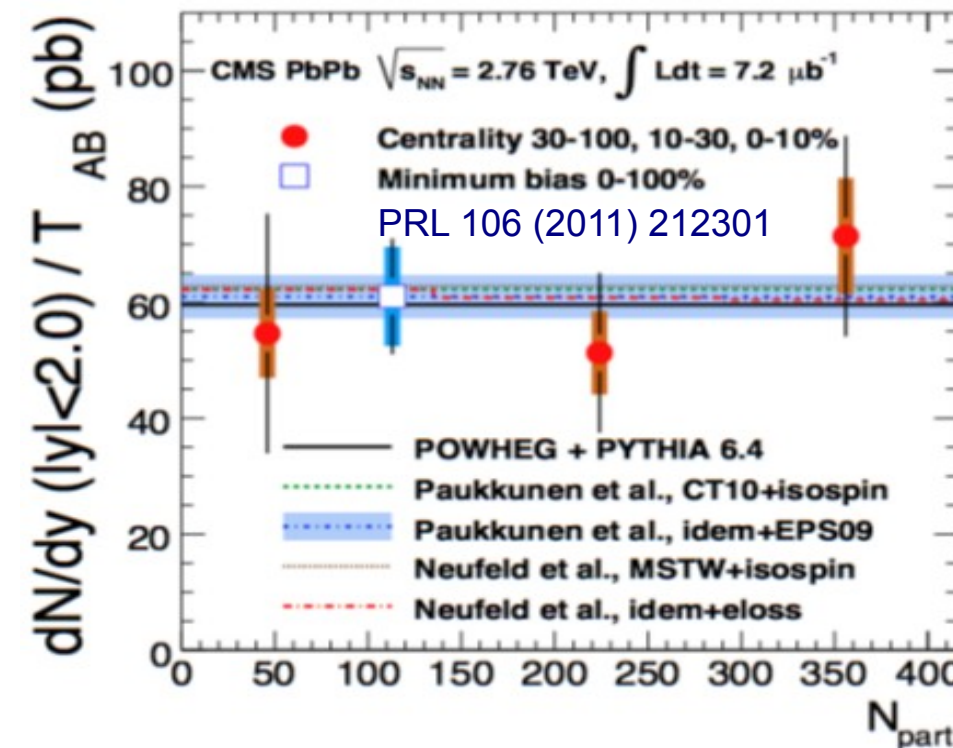
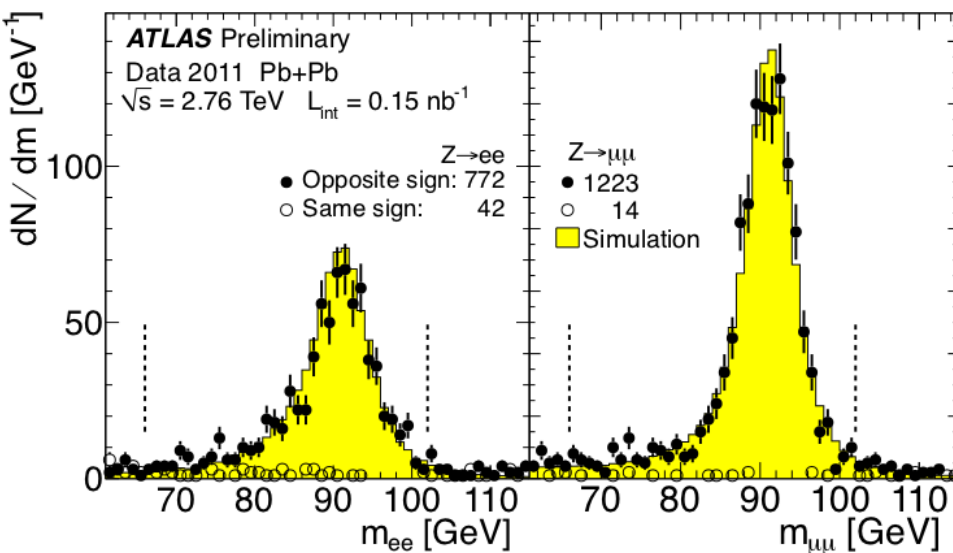


- Good agreement between data and NLO
- Small nuclear modification in probed x, Q^2 region (Nuclear PDF uncertainties $\pm 30\%$)

Isolated photons follow expected scaling ie. isolated photon $R_{AA} \sim 1$

Control probe: Z bosons

46

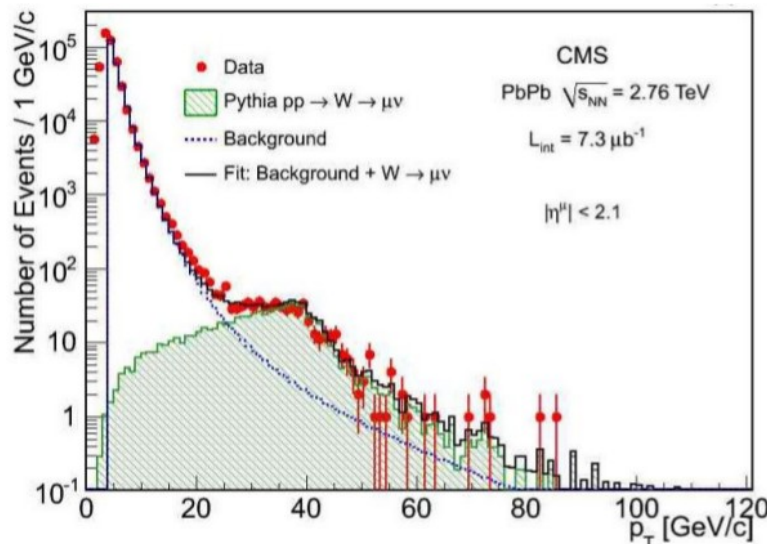


Scaled Z yields flat and consistent with NLO for all centralities:
 $R_{AA} = 1 \pm 0.16 \text{ (stat)} \pm 0.14 \text{ (sys)}$
(pp reference from Powheg)

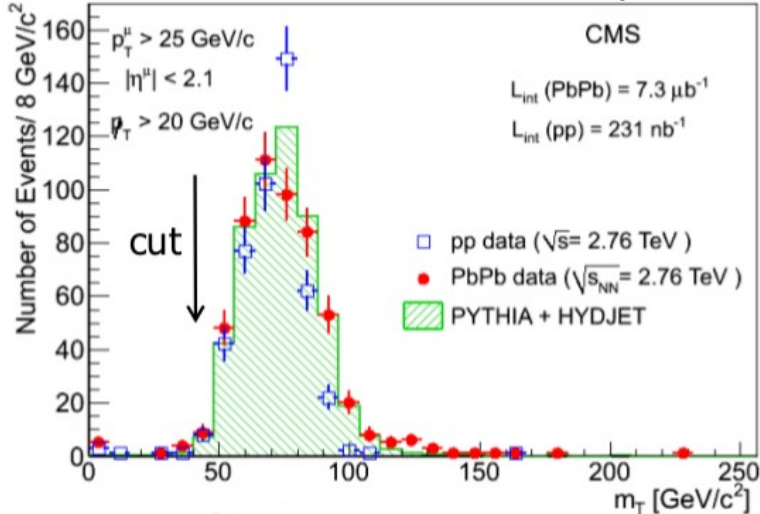
Control probe: W bosons

47

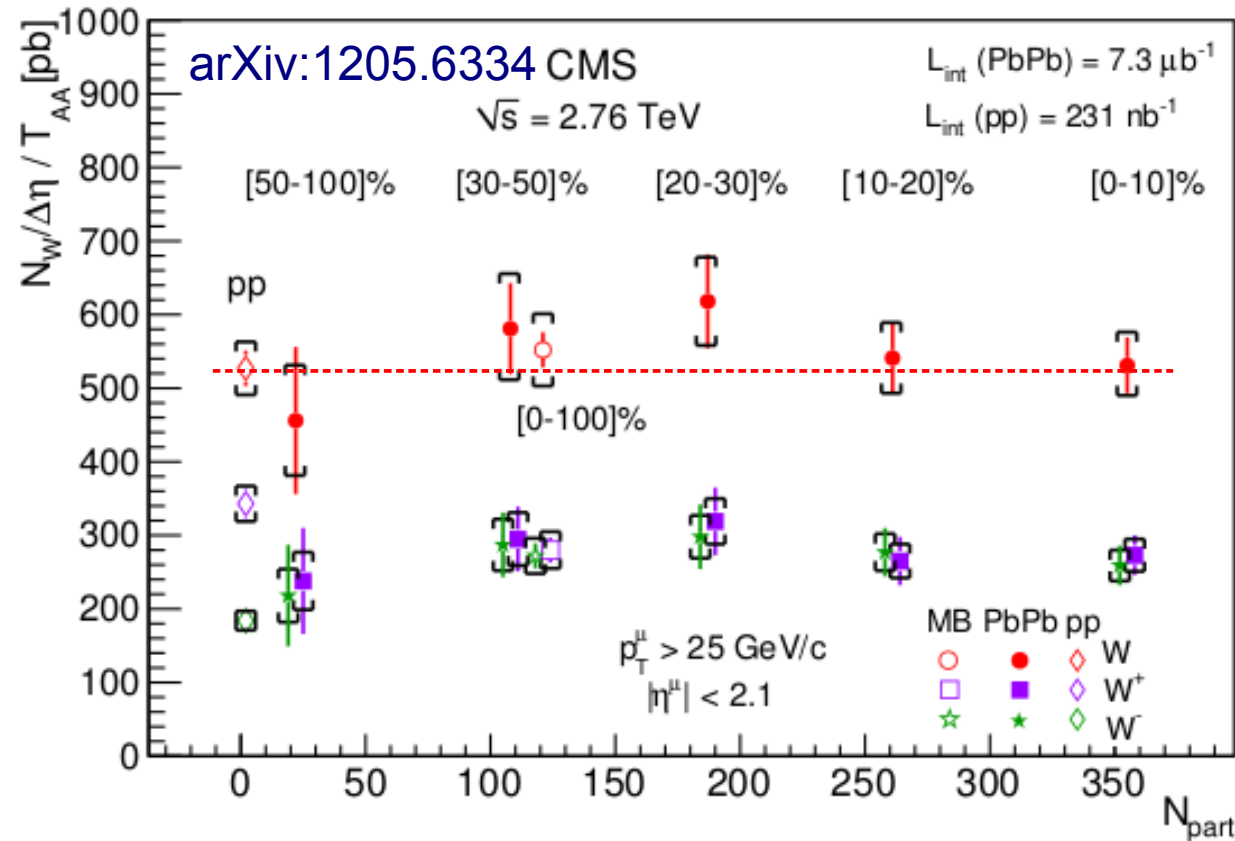
Fit template (Pythia) + bkg model



Transverse mass analysis



Also ATLAS-CONF-2011-78



Yields on W^+ and W^- separately reflect the different u and d quark content in Pb and p

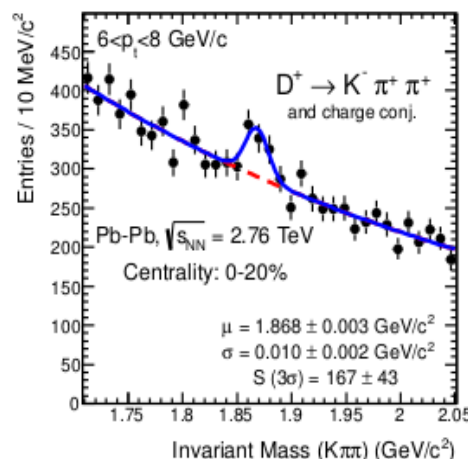
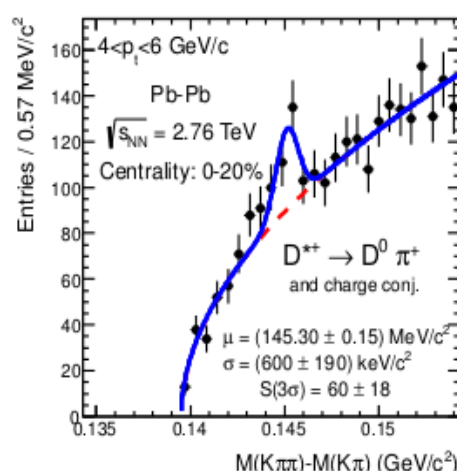
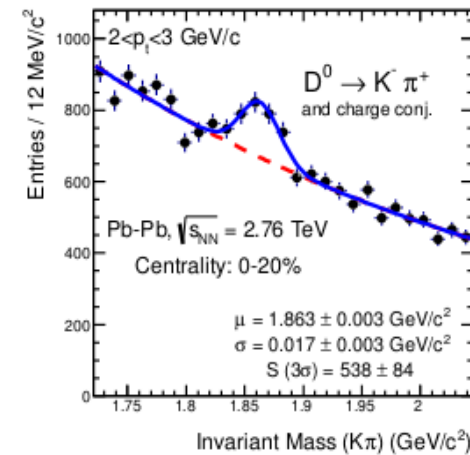
Within uncertainties, no dependence of the binary scaled W yields on centrality:
 $R_{AA} = 1.04 \pm 0.07 \text{ (stat)} \pm 0.12 \text{ (sys)}$

Heavy-quark probes: D and B mesons

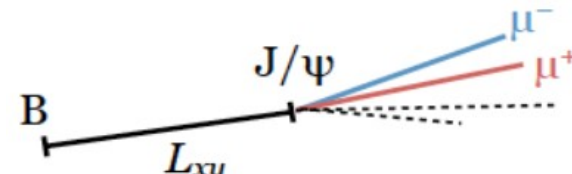
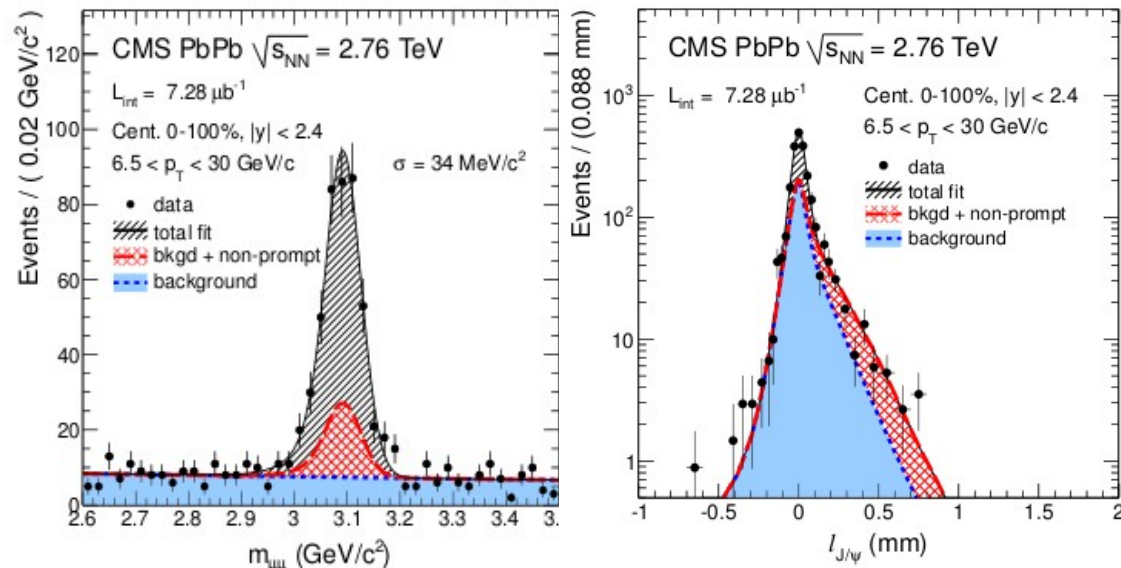
48

D mesons reconstructed from displaced vertices in 3 invariant mass channels. Contribution from B subtracted with FONLL.

ALICE, arXiv:1203.2160



B mesons via secondary J/ ψ :
CMS, JHEP 1205 (2012) 063

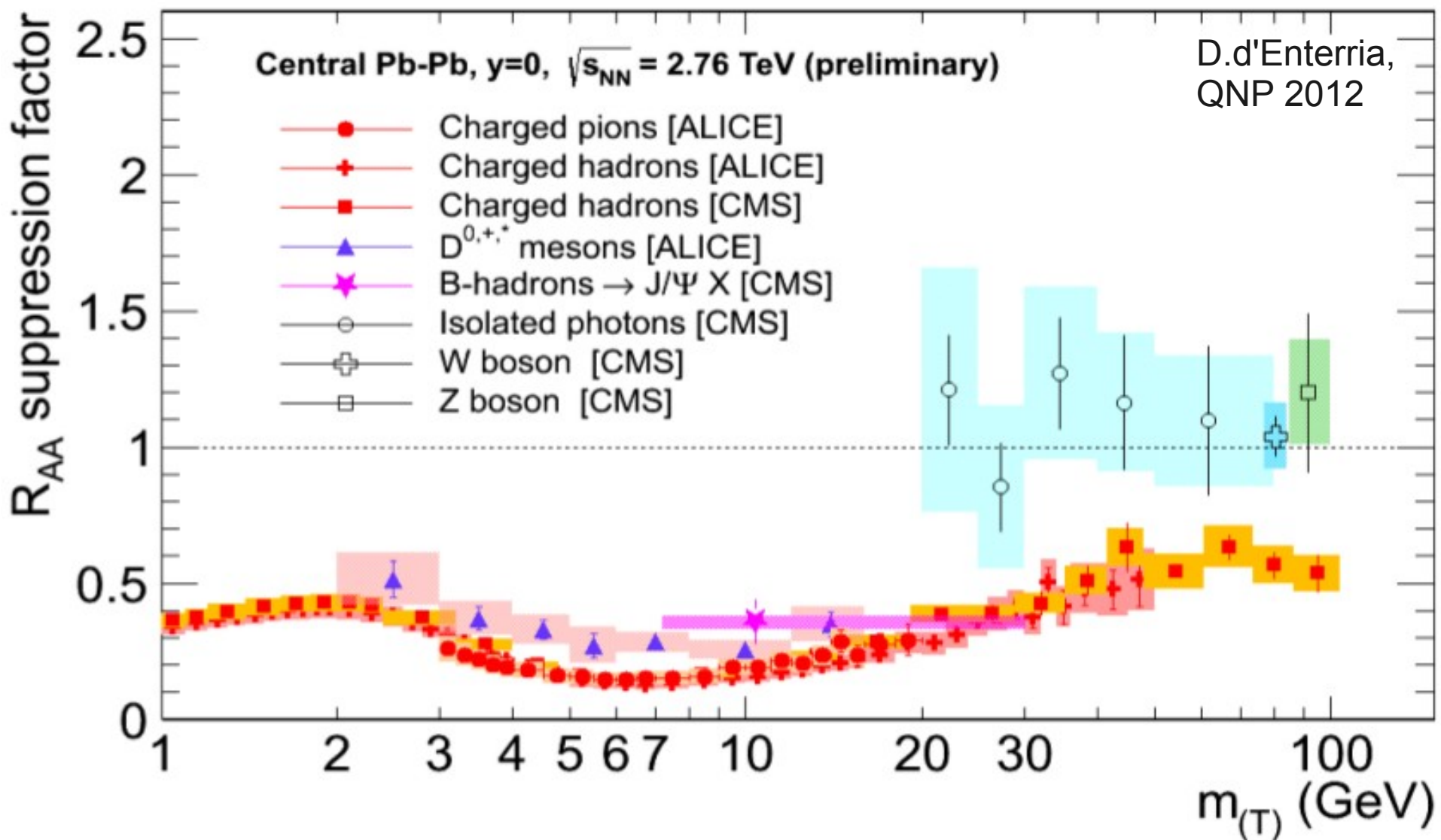


Clean separation of 2nd vertex
for J/ ψ with $p_T > 6.5 \text{ GeV}/c$

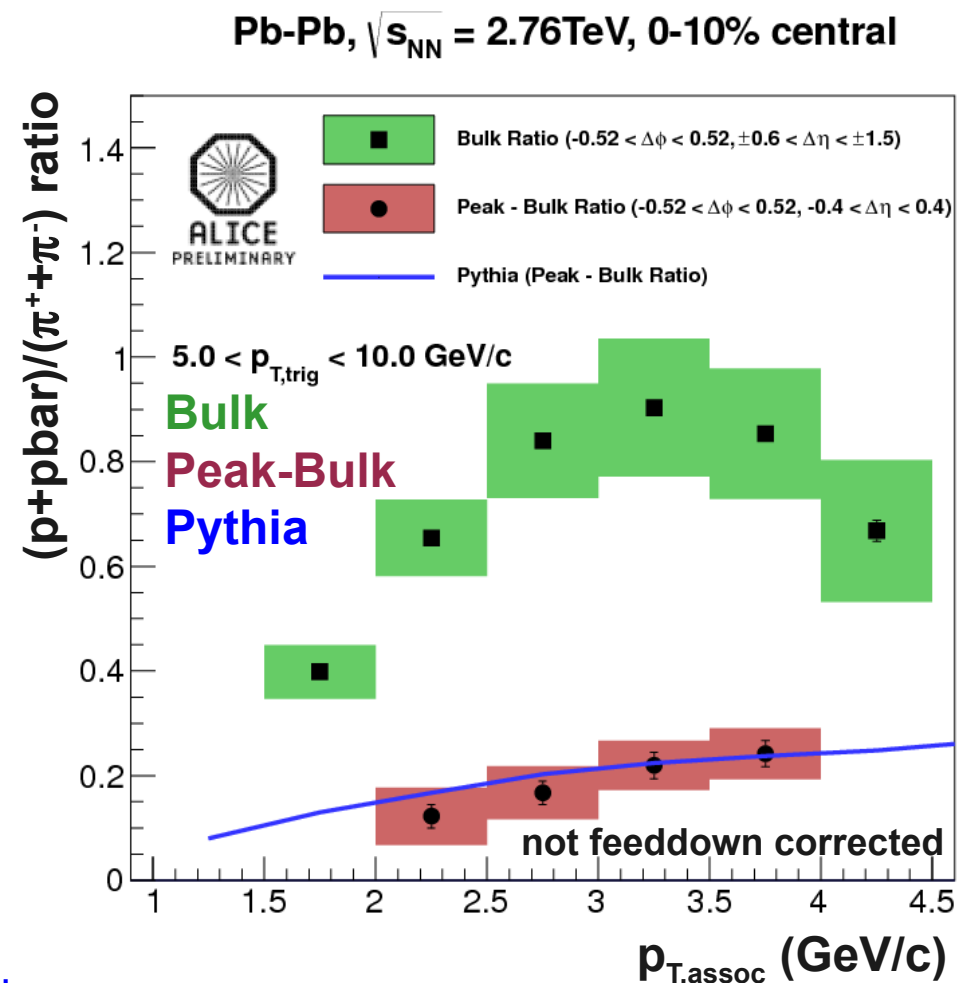
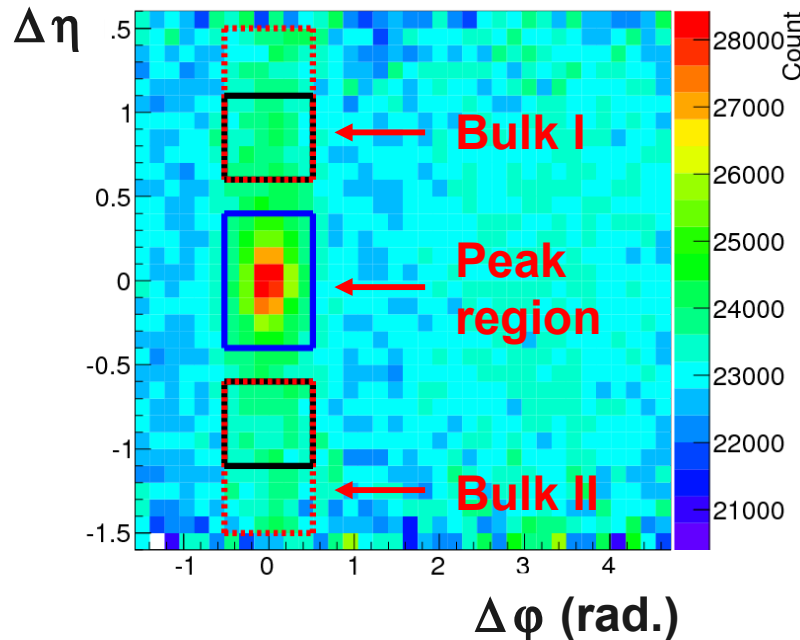
Also recently presented (not discussed here):
ATLAS HF muon, mid-rapidity (ATLAS-CONF-2012-050)
ALICE HF muon, forward (arxiv:1205.6443)

Summary of single particle probes

49



Near-side di-hadron correlations: p/π ratio 50



- p/π ratio in the bulk is consistent with inclusive p/ π ratio
 - NB. Inclusive ratio in 0-5% and feeddown corrected
- p/π ratio in peak - bulk is consistent with ratio from Pythia (6.4 default tune)
- No evidence for medium-induced modification of jet fragmentation ($R \sim 0.4-0.5$) in this p_T regime